

Review on spin-wave RF applications

Khrystyna O. Levchenko^{1*}, Kristýna Davidková^{1,2}, Jan Mikkelsen³, and Andrii V. Chumak^{1†}

¹ Faculty of Physics, University of Vienna, 1090 Vienna, Austria.

² Vienna Doctoral School in Physics, University of Vienna, 1090 Vienna, Austria.

³ Department of Electronic Systems, Aalborg University, 9220 Aalborg, Denmark

Email: *khrystyna.levchenko@univie.ac.at, †andrii.chumak@univie.ac.at

Abstract—This review explores the progress of spin-wave technology, emphasizing magnonics as a potential solution to modern challenges in radio frequency (RF) communication systems. To ensure clarity, the first two sections of the review reiterate premises of the magnonics, outline key milestones in spin-wave research, briefly review the state-of-the-art for technology and materials, as well as highlight potential directions for future developments. The third section is dedicated to spin-wave RF applications developed over the past 50 years, focusing on selected passive fundamental devices (filters, power limiter, delay lines, phase shifters, directional couplers, resonators, etc) and their operating principles. In the last section, the review further discusses the main advantages of spin-waves for RF applications while highlighting potential concerns, such as insertion losses, linearity and power capacity. Finally, potential solutions to address these challenges are proposed.

CONTENTS

I	Introduction	1
I-A	State-of-the-art and challenges of the commercial mobile communication system	1
I-B	Milestone history of spin-wave research and technology	3
I-C	Core principles and key concepts of spin-wave technology	5
I-C1	<i>Basics of magnonics</i>	5
I-C2	<i>Spin-wave parameters important for applied science</i>	6
I-C3	<i>Choosing magnonic materials</i>	7
II	Modern magnonics: general overview	7
II-A	Current state of the magnonic field	7
II-B	Vectors of the cutting-edge developments	7
II-B1	<i>Notable progress in microwave transducers design</i>	7
II-B2	<i>Advancement in understanding of the nonlinear spin-wave physics</i>	8
II-B3	<i>Nanoscaling</i>	9
II-B4	<i>Micromagnetic simulation tools for spin-wave dynamics</i>	9
II-B5	<i>Machine learning and inverse design</i>	9
II-B6	<i>Non-reciprocity of spin waves</i>	10
II-B7	<i>Quantum magnonics</i>	10
II-B8	<i>Alternative materials</i>	10

III	Spin-Wave technology for RF applications	11
III-A	SW filters	12
III-B	SW channelizer	16
III-C	SW phase shifters	16
III-D	Delay lines	18
III-E	Frequency selective limiters and signal-to-noise enhancers	18
III-F	Resonators	21
III-G	Directional couplers	22
III-H	Selected spin-wave RF patents	22
IV	Advantages and challenges of spin-waves for RF applications	23
IV-A	Advantages	23
IV-B	Areas of concern in RF applications	25
IV-C	Strategies to overcome the concerns in RF magnonics	26
	References	28

I. INTRODUCTION

A. State-of-the-art and challenges of the commercial mobile communication system

With each new generation of mobile communication — from GSM through 5G and the upcoming 6G — there has been an increased focus on bandwidth and functionality, pushing manufacturers to address growing complexities. Initial 5G deployments in the European Union relied on standard frequency bands, specifically 694–790 MHz for low-band and 3.4–3.8 GHz for mid-band, but the need for faster data rates and lower latency has driven the shift toward high-band frequencies. The EU’s 5G high-band, spanning 24.25–27.5 GHz, offers greater bandwidth, enabling high-speed data transfer and reduced latency, which is essential for applications like IoT, autonomous vehicles, and high-definition streaming.

Currently, a fundamental and widely adopted telecommunications technology is the Multiple-Input Multiple-Output (MIMO) RF system concept. A MIMO RF system implements a number of parallel RF channels, each consisting of a number of passive and active elements, that connect to multiple antennas (Fig. 1) to simultaneously transmit and receive multiple data streams. Key performance metrics for such systems are power efficiency of the power amplifier module, insertion loss of all passive blocks between the amplifier output and the antenna, manufacturing complexity, size and costs. The

utilization of MIMO systems has provided a significant boost in system capacity. A boost that is needed for current and future communication system generations.

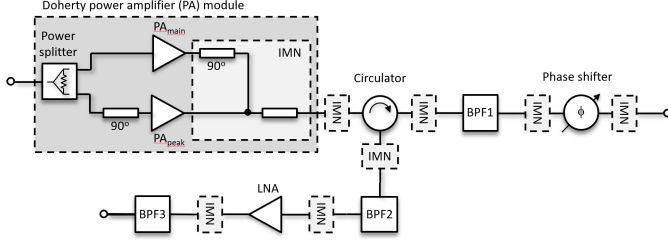


Fig. 1: Illustration of a generic radio channel front-end architecture, including typical functional blocks: **Doherty PA** - type of a power amplifier module, which consists of a power splitter (splits the incoming signal into multiple signals with even or uneven power levels) - PA_{main} and PA_{peak} ; **IMN** - impedance matching network for efficient power transfer between the signal source and the power amplifier; **circulator** - device to isolate the high power transmitter from the sensitive receiver; **BPF(1/2/3)** - bandpass filter that allows signals within a designated frequency band to pass; **LNA** - amplifier that enhances weak incoming signal from the antenna while introducing minimal additional noise; **phase shifter** - unit that steers the direction of a signal transmitted or received by the antenna.

However, operation at higher frequencies presents significant design challenges, including increased signal loss, the need for advanced materials, greater power consumption to maintain signal quality, etc.

The performance of active components like amplifiers, mixers, modulators, etc (units that require external power to process signals¹), in terms of size and signal transmission, is largely driven by semiconductor technology. At this stage of development, magnonics can not compete with the semiconductor's functionality, especially in terms of insertion losses, but might be a long-term candidate from the perspective of minimized power dissipation/consumption.

With the many RF channels operating in parallel, power efficiency of MIMO systems becomes critical, especially at 6G frequencies where losses increase. The combined power dissipation of such MIMO systems require high thermal dissipation performance, which calls for inclusion of intricate cooling systems. This increases the overall system form factor as well as reduces the overall power efficiency of the combined system. Here, isolator-based magnonics has potential as it would inherently solve this bottleneck problem.

Passive components, such as filters, couplers, power limiters, phase shifters, transmission lines, etc (units for directing and conditioning RF signals), on the other hand, are more 'open' to new technologies and materials due to accumulated pending issues that cannot be solved with current MIMO approaches. Similarly to active MIMO components, passive MIMO components at frequencies beyond mid-5G band suffer from higher signal attenuation, interference, mutual coupling, increased complexity, etc. Yet, unlike active components, modern monoblock ceramics technology, typically used in MIMO

for filters, delay lines and phase shifters, can not offer much improvements for higher frequencies. Also, with state-of-the-art ceramics the insertion losses of such mono-block filters are limited by the electric conductivity of the silver coating. As a consequence a physical limitation for down-scaling the size is rapidly approaching. Fragility and limited tuning capability of ceramic devices further restrict their suitability for modern communication systems, rendering them inefficient for future RF applications. This review focuses primarily on passive spin-wave RF devices.

Furthermore, widely-used PIN diodes-based power limiters face challenges, such as slow response times and enhanced noise at high GHz frequencies. Additionally, as most MIMO passive units are based on micro- and millimeter-wave technology, they take the largest area of combined radio front-end and are hard to scale down.

Consequently, most of the conventionally used filters, multiplexers and delay lines for wireless data transmission systems are based on the compact Surface Acoustic Waves (SAW) technology [1], [2] that enabled the compact multi-band telecommunication devices to meet current (LTE, 5G low band) demands. Yet, the frequency limitations, dictated by the increased insertion loss above 3 GHz, still persist [3], as well as the exposure limitations of interdigitate transducers (IDTs)[1], [3]. **SAW technology can not meet the demands of a reliable operation over the whole frequency range of the current 5G communication technology.** The frequency bottleneck is partially addressed by the Bulk Acoustic Waves (BAWs) technology, which allows for a reliable operation up to 6-10 GHz. However, the high-frequency range (30 GHz) remains largely unexplored. Currently, the main impediments are increased damping and inefficient energy transfer between the transducer and the bulk acoustic wave within the propagation medium at higher frequencies, strict requirements for BAW isolation from the substrate to prevent unwanted energy dissipation, and the subsequent complexity of the fabrication process [3]. Unlike SAW devices, BAW filters require acoustic waves to travel through the bulk of the material, which can lead to difficulties in maintaining signal integrity and resonance efficiency at high frequencies (more on device-specific challenges in *Section II A*).

As performance trade-offs between BAW and SAW RF devices still leave room for improvement, manufacturers are concurrently exploring new, alternatives. Spin-wave technology presents a promising solution, addressing several of the limitations of traditional devices: (1) **a wide frequency range spanning from < 1 GHz to THz** [4]; (2) **compatibility with the industry-standard fabrication process** (photolithography) for spin-wave transducers; (3) **inherent isolation**, as spin waves are naturally confined within the magnetic material and do not propagate into the substrate or adjacent filters, unlike SAWs; (4) **rich nonlinear functionalities**, such as power limiting and signal-to-noise ratio enhancement. Furthermore, spin waves offer enhanced **flexibility**, as their dispersion characteristics can be controlled through magnetization orientation, applied current, or field, enabling the development of reconfigurable RF devices with timescale control on the

¹Some RF units, depending on the design, can be realized either as active or as passive elements, e.g., filters; phase shifters.

order of nanoseconds (more on the spin-wave advantages in Section II A).

In this review, we aim to engage both the magnonic and RF engineering communities by examining the challenges of selected modern RF telecommunication elements through the lens of spin-wave technology.

B. Milestone history of spin-wave research and technology

A **spin wave (SW)** represents a propagating collective excitation of magnetic moments in magnetically ordered materials. The quanta of these excitations are known as **magnons** [5], [6], [7]. The emerging field of research that investigates information transport and processing through spin waves, as an alternative to or in conjunction with the electric currents, is known as **magnonics** [8], [9]. The integration of magnonic principles within spintronics, which traditionally focuses on electron-based spin currents, has led to the development of **magnon spintronics**. This interdisciplinary field encompasses magnon-based components that handle both analogue and digital data, as well as devices that facilitate conversion between magnonic subsystems and electron-based spin and charge currents. Although the study of spin-wave phenomena is less than a century old, it has already become a significant area of research, leading to numerous advanced applications. These applications serve as potential alternatives to CMOS [10] technology and pave the way for innovative fields such as magnonic neuromorphic computing [11], [12], [13], quantum computing [14], [15], [16], etc.

The timeline of milestone discoveries

- **1919:** The phenomenon of **ferromagnetic resonance (FMR)** was first experimentally discovered independently by Griffiths and Zavoisky, while its first comprehensive theoretical description was given by Kittel in 1948 [17].
- **1921:** Stern and Gerlach performed the first experimental **observation of the electron spin** [18]. Silver atoms, while passing through an inhomogeneous magnetic field, were deflected up or down by the same amount, indicating a directional quantization of quantum mechanical angular momentum – spin.
- **1928:** **Theoretical equation for spin 1/2 particles** was developed by Dirac, showing positive and negative energy states [19], [20].
- **1929:** Spin waves were predicted by Bloch and named as such due to the relation to collective excitations of the electron spin system in ferromagnetic metals and insulators [21]. Early experimental evidence of spin waves came from measurements of thermodynamic properties of ferromagnets, in particular, the temperature dependence of their saturation magnetization M_s [8]. The famous $T^{3/2}$ Bloch law is an indirect confirmation of the existence of spin waves [22].
- **1935:** Development of the theory on the relaxation dynamics of the magnetization vector by Landau and Lifshitz, which led to the development of the fundamental equation of magnetization dynamics – **Landau-Lifshitz-Gilbert equation (LLG)** [23], [24].
- **1940-56:** Holstein and Primakoff [25], and later Dyson [26], introduced **quanta of spin waves called magnons**. They predicted that magnons should behave as weakly interacting quasiparticles obeying the Bose-Einstein statistics [8]. The subfield of magnetism associated with the quantum magnetic dynamic phenomena was hence called **magnonics** [8]. Nowadays, similarly to electronics, magnonics is not limited by the scale of its medium/quanta but rather covers a broad field of magnetism connected with spin waves.
- **1946:** The **first direct observation of spin waves** by Griffiths [27] via the FMR spectroscopy for the case of uniform precession (non-propagating spin wave with wavevector $\mathbf{k} = 0$). The pioneering experiments on the propagating spin waves $\mathbf{k} \neq 0$ were performed two decades later by Fleury et al., using Brillouin light scattering (BLS) spectroscopy [28].
- **1952:** **Microwave (MW) magnetic devices** debuted on the applied scene with Hogan's work [29] on the gyrator using Faraday rotation. This low-loss (7 dB) broadband device had potential for one-way transmission systems, microwave circulators, microwave switches, electrically controlled variable attenuators and modulators.
- **1952-57:** The **first non-linear measurements** were reported by Bloembergen and Damon [30], and Bloembergen and Wang [31] at the ferromagnetic resonance of the material, while 'pumping' high-power radio frequency (RF) field transverse to the applied magnetic field. As explained by Suhl [32], [33], certain SW modes are parametrically induced when the MW field creates a uniform precession of the magnetization and, simultaneously, once the MW power exceeds a certain threshold. Nonlinear physics peaked in the 80s, but is already making a swift comeback to cutting-edge research since it provides valuable guidelines for the efficient generation and amplification of SWs on the nanoscale – a key to developing advanced magnonic networks.
- **1956:** Synthetic dielectric ferrimagnet **yttrium iron garnet ($\text{Y}_3\text{Fe}_5\text{O}_{12}$ – YIG)** was first fabricated by Bertaut and Forrat [34]. This is an indispensable material for magnonics, akin to silicon in semiconductor physics, due to the wide range of accessible frequencies (MHz - GHz) the narrowest known ferromagnetic resonance linewidth and the lowest spin-wave damping. Therefore, it is widely used up till now in RF technology (microwave filters, Y-circulators, microwave generators, etc. [35]) and experimental physics for studying new effects and phenomena in magnonics [34]. The Gilbert damping parameter of YIG (both bulk and ~ 100 nanometer-thick film) reaches values of about 10^{-5} , allowing microwave filter development with a high-quality factor (Q) in the order of 10^5 . The operating principle of such YIG devices is based on the use of non-propagating FMR or on the modification of the properties of the electromagnetic wave (EM waves or EMWs) propagating in a medium with a YIG sphere.

- **1959:** The first publication on the characteristics of ferrite RF power limiters by Uebele [36]. Several techniques for increasing the insertion loss of ferrite-loaded waveguide structures at high RF power levels have been presented, and the operating characteristics of a ferrite microwave limiter have been described.
- **1960:** The discovery of magnetostatic surface waves (MSSWs, alternatively named Damon-Eshbach SWs) by Eshbach and Damon, and characteristic modes of a thin slab magnetized in its plane are obtained in the magnetostatic limit [37]. It is found that the slab's magnetostatic mode spectrum is bounded by the same frequency limits as for the spheroid. In the slab, however, the mode configuration clearly changes from a volume distribution to a surface wave as the frequency is increased above the extrapolated spin-wave region.
- **1970-80s:** Peak of the high-profile investigations dedicated to the development of the **spin-wave passive and active RF devices** [38], [39]. One of the most broad and excellent overviews on state of the **magnetostatic wave (MSW) RF devices** was given by the series of authors in *IEEE* 76(2) [40], [41], [42], [43], [44], where each of them highlighted a different aspect of the field. Among the discussed topics were spin-wave based filters [40], transducers, delay lines and directional couplers [42], phase shifters, parametric amplifiers and signal-to-noise enhancers [43], circulators [44], etc. Details on the devices and concepts are provided in further sections. After this peak, some groups further optimized the operating characteristics of spin-wave RF devices, e.g., **reduced the insertion loss of RF filters to 2.5 dB** [45].
- **2004-now:** The idea of coding binary data into the spin-wave amplitude was first stated by Hertel et al., [46] and opened the direction of **the digital data processing using spin waves** [47]. Micromagnetic simulations revealed that MSSWs change their phase as they pass through the domain walls. Experimental development of **spin-wave logic** started with the work of Kostylev et al. [48]. Following this idea, Schneider et al., realized a proof-of-principle XNOR logic gate and a universal NAND logic gate [49]. The ability to create NOT, NOR and NAND logic gates was demonstrated using numerical simulations and experimental studies by Lee et al. [50]. In the approaches discussed above, data was coded into SW amplitude (a certain amplitude defines logic "1", zero amplitude corresponds to logic "0"). Alternatively, Khitut et al., [51], proposed to use the SW phase for digitizing information instead of the amplitude, which allows for a trivial embedding of a NOT logic element in magnonic circuits, and enables the realization of a **majority gate** in the form of a multi-input SW combiner [51]. The advantage of such a device is in the ability to operate with spin waves of different wavelengths simultaneously, paving the way towards the single chip parallel computing [52]. An experimental prototype of a majority gate based on a macroscopic YIG structure was shown later by Fischer et al., [53] and a **chip-ready in-line majority gate** was developed by imec [54]. A **magnon transistor**, which opened a way for all-magnon data processing of digital data, was discovered by Chumak et al. [55]. Following this path, a **magnonic directional coupler for integrated magnonic half adders**, designed based on the single-mode nanoscale YIG waveguides, was first simulated and later experimentally realized by Wang et al. [10]. The proposed concept developed with 30-nm technology can have a footprint comparable to a 7-nm CMOS half-adder, with $\approx 10\times$ smaller energy consumption.
- **2005-now:** A new promising direction of the universal magnonic units – **magnonic crystals** – started to gain weight in the field [14], [56]. Magnonic crystals are the artificial magnetic materials with a spatially periodic variation of properties for versatile applications, especially aiming at RF, logic and data-processing (e.g., filters [57], [58], sensors [59], [60], transistor [55], logic gate [61], etc). Initially, periodic structures were studied in particular for the realization of MSW filters and resonators [62]. Since then, a significant progress was made in developing versatile types of magnonic crystals, improving their functionality, and understanding the underlying physics [56], [14].
- **2008-now:** **The miniaturization of magnonic structures from millimeter-scale lateral dimensions to micrometer-scale** has advanced for both metallic systems [63], [64], [65], [66] and YIG films [67], [68], [69]. Further progress in scaling YIG structures to sub-micrometer dimensions was enabled by the revolutionary development of high-quality, nanometer-thick YIG films fabricated using liquid-phase epitaxy (LPE) [70], [71], [72], [73], pulsed laser deposition (PLD) [74], [75], [76], [77], [78], and sputtering [79], [78], achieving thicknesses as small as sub-10 nm. In nanoscopic YIG conduits with an aspect ratio of thickness to width approaching unity [80], [81], exchange unpinning effects emerge, resulting in spin-wave mode quantization along the frequency axis and enabling operation in a single-mode regime. This single-mode operation minimizes parasitic scattering into higher width modes, significantly advancing applied nanomagnonics [10], [12].
- **2016-now:** **Optimization and development of new types of spin-wave transducers.** Since the efficiency of spin-wave transducers defines the energy consumption in magnonic devices for digital data processing and the insertion loss in RF devices, an intensive investigation of improved or novel types of transducers has been carried out [82], [83], [84], [85]. In particular, the use of spin-orbit torque [86] has been employed to improve the efficiency of the transducers [87].
- **2020:** The research **revival of spin-wave RF applications triggered by 5G technology requirements.** On-chip MSW resonator [88] and stopband filters [89] were demonstrated. In addition, high-power microwave pulse measurements were performed in the absorptive-type microstrip YIG power limiter [89]. A cutting-edge nanoscale three-in-one RF concept was recently devel-

oped (frequency-selective limiter, filter, delay line), which further pushes the boundaries of applied magnonics. Considering the fast market growth and technological requirements of 5G technology, the inability of surface acoustic wave technology to meet the requirements in the > 3 GHz frequency range, together with the obstacles of bulk acoustic wave RF application, SW technology, as an alternative solution, is rapidly attracting interest.

- **2020:** Emergence of a novel **quantum magnonics** field, that converged previous researches into a clear-sighted direction. Most probably, an article by Lachance-Quirion et al., [90] was a kick-off moment, as it showed how to detect a single magnon with a quantum efficiency of up to 0.71 using an entangle hybrid structure of a superconducting qubit and a ferrimagnetic crystal. This proof-of-concept experiment provided the basis for a wide range of future applications, like quantum magnonic sensing or computing. Currently, a key focus in quantum magnonics is the exploration and utilization of propagating magnons, as opposed to standing magnons, to enable dynamic quantum systems with enhanced functionality [91], [92]. One of the most prominent subfields of quantum magnonics is hybrid magnonics, which explores the coupling of magnons with other physical systems, such as photons, phonons, or qubits, thereby providing a platform for the development of novel quantum technologies for quantum information, wave-based computing, and sensing applications [93], [94], [95], [15], [96], [97].
- **2021:** The use of **inverse design and machine learning in magnonics** enables modern AI-based tools for solving versatile tasks in the field. In particular, magnon power switches, (de-)multiplexers and Y-circulators have been demonstrated [98], a neuromorphic computing unit for the vowel sound recognition has been reported [13] and engineering of spin-wave pulses has been developed [98] using inverse design. A major breakthrough in the field was recently demonstrated by Zenbaa et al., with a first experimental reconfigurable, lithography-free, and simulation-independent inverse-design device capable of implementing diverse RF components [99]. The power of AI has enormous potential, and the field of inverse-design magnonics is developing swiftly.

C. Core principles and key concepts of spin-wave technology

1) *Basics of magnonics:* This Section is based upon the articles by Serga et al., [9] and Chumak [4]. All information is the subject of their intellectual property. In the unstructured, continuous magnetic system, the magnetization precession \mathbf{M} is described through the Landau-Lifshitz-Gilbert equation of motion:

$$\frac{d\mathbf{M}}{dt} = -\gamma\mu_0(\mathbf{M} \times \mathbf{H}_{\text{eff}}) + \frac{\alpha}{M_s} \left(\mathbf{M} \times \frac{d\mathbf{M}}{dt} \right), \quad (1)$$

where γ is the gyromagnetic ratio - constant of proportionality between the magnetic moment and the angular momentum, μ_0 - permeability of free space, \mathbf{H}_{eff} - effective magnetic field, α

- dimensionless Gilbert damping factor, M_s is the saturation magnetization.

Solutions to Eq. 1 in the macrospin approximation are uniform and non-uniform modes of spin magnetic moments precession. The first term corresponds to the in-phase precession of individual spins and leads to the Kittel equation for ferromagnetic resonance (FMR). The last term describes the spin waves – spins oscillating at the same frequency but with different phases.

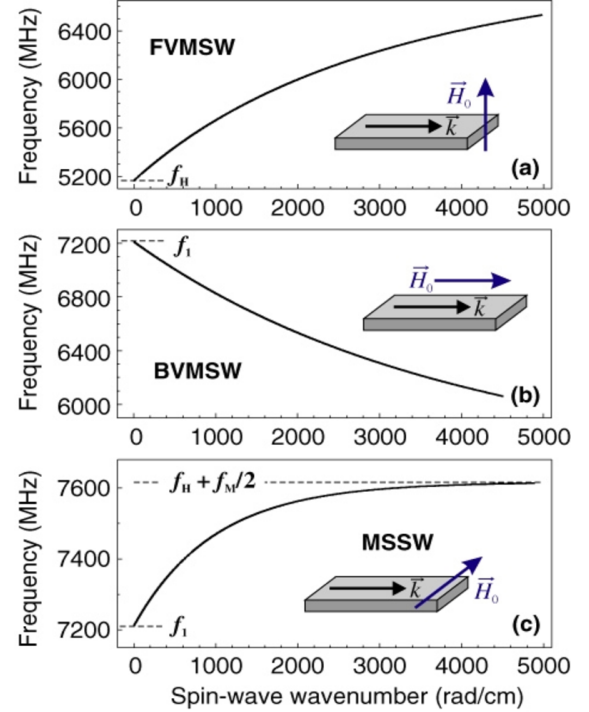


Fig. 2: Calculated dispersion characteristics (lowest order thickness modes) using Eq.(1-3) for (a) Forward volume magnetostatic spin wave (FVMSW), (b) Backward volume magnetostatic spin wave (BVMSW), (c) Magnetostatic surface spin wave (MSSW). Bias magnetic field $B = 184.5$ mT, saturation magnetization $M_s = 1750$ G, film thickness $d = 5\mu\text{m}$. Adapted from [4].

Three fundamental modes of SW can be excited in a thin magnetic waveguide, as shown in Fig. 2. The spin-wave mode type depends on the direction of the applied magnetic field with respect to spin-wave propagation. These SW modes are distinguished by different dispersion relations, $f(k)$, i.e. the dependence of the SW wave frequency f on its wavevector k (wavenumber); see Fig. 2:

- **Forward Volume Magnetostatic Spin Wave (FVMSW),** For FVMSW, the magnetic film is magnetized normally concerning the layer surface; see the Fig. 2(a). The dispersion relation for FVMSW is of the form

$$f = \frac{\gamma}{2\pi} \sqrt{B \left[B + \mu_0 M_s \left(1 - \frac{1 - e^{-kd}}{kd} \right) \right]}, \quad (2)$$

where d is the film thickness, which mostly determines the slope of the dispersion relation. An important distinguishing feature of FVMSWs is the dispersion isotropy in the plane of

the film, as the spin waves always propagate normally to the applied bias field B .

- **Backward Volume Magnetostatic Spin Wave (BVMSW)**, For BVMSW, the magnetic film is magnetized in-plane, and the applied film is parallel to the SW propagation; see the Fig. 2(b). It is a volume mode, which means that the amplitude of the magnetization precession has a cosinusoidal distribution across the film thickness. The main peculiarity of BVMSW is the negative slope of the dispersion curve and, consequently, the negative group velocity. This unusual physics implies that the phase and group velocities of the waves are counter-propagating, and an increase in k is associated with a decrease in the SW frequency. BVMSWs follow a dispersion relation:

$$f = \frac{\gamma}{2\pi} \sqrt{B \left[B + \mu_0 M_s \left(\frac{1 - e^{-kd}}{kd} \right) \right]}. \quad (3)$$

- **Magnetostatic Surface Spin Wave (MSSW)**, For MSSW, the magnetic film is magnetized in-plane, and the applied film is parallel to the SW propagation; see the Fig. 2(c). Unlike backward and forward volume waves, MSSWs (or Damon-Eshbach spin waves) are localized to one surface of the film in which they propagate. The distribution of precessional amplitude across the film thickness is exponential, with a maximum at one surface of the film. MSSW dispersion is calculated as:

$$f = \frac{\gamma}{2\pi} \sqrt{B(B + \mu_0 M_s) + \frac{\mu_0^2 M_s^2}{4} (1 - e^{-2kd})}, \quad (4)$$

In the simplest case, there are two main contributors to the SW energy: **weak, long-range dipole-dipole** and **strong, short-range exchange interactions** [6], [7], see Fig. 3.

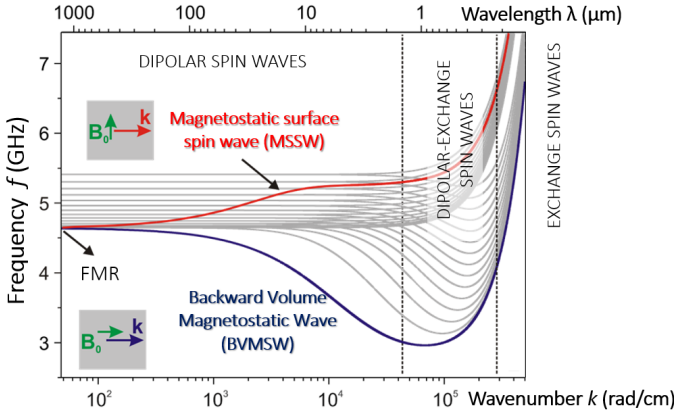


Fig. 3: Dispersion relations of in-plane magnetostatic spin waves and a change of dominating interactions (dipolar, dipolar-exchange, and exchange) relative to the increase in wavenumber k . Adapted from [4].

In the magnetostatic regime, the dipolar interaction between spins is dominant since the wavelength λ ($k = 2\pi/\lambda$) here is much longer than the exchange length. As a result, the dispersion relations for in-plane magnetized films are strongly anisotropic (directionally dependent) due to the dipolar interaction. Hence, the dispersions of SWs are complex and

significantly different from the well-known linear dispersion of light or sound in uniform media. For certain devices, magnetic anisotropy can serve as an additional degree of freedom, offering potential advantages, or it may play a minimal role. However, for most data-processing and RF applications, the anisotropy and relatively low group velocity (processing speed) of magnetostatic spin waves (SWs) could pose limitations.

2) *Spin-wave parameters important for applied science:* Important spin-wave parameters (group velocity, v_{gr} , lifetime, τ , mean free path, l_{free} , etc.), can be obtained from an analysis of the dispersion relations:

- The **group velocity** of a spin wave is defined as $v_{gr} = 2\pi \cdot \delta f / \delta k$ and can be found by differentiating Eq. (2) or Eq. (3). As mentioned above, the group velocity is negative for the BVMSW with small wavenumbers, then it passes through the zero value in the MSSW region, and increases monotonically in the exchange region reaching values of around 20 km/s (in YIG waveguide of width 1 μm and 100 nm thickness, magnetized along with 100 mT bias magnetic field [4]). From the application point of view, SW group velocity v_{gr} is important as it dictates the speed of data transfer and defines delays between different magnonic elements. Hence, in the simplest case, a clock rate of the device is limited by the SW group velocity, which should also be maximized.

- The main parameters that determine the **lifetime or relaxation time of spin waves**, τ , are the SW frequency, f , and Gilbert damping constant, α , of a magnetic material ($1/\alpha$ defines approximately the number of precession periods before the wave vanishes). The lifetime of the uniform precession mode in an infinite medium or a sphere is simply expressed as $\tau_0 = 1/(\alpha \cdot 2\pi f) = -2/(\gamma \mu_0 \Delta H)$ [7]. A general expression for the lifetime appropriate for the particular mode and geometry is $\tau_k = -1/\text{Im}\{2\pi f\} = \tau_0 \cdot \delta(2\pi f_0) / \delta(2\pi f)$, where $\delta(2\pi f_0) = -\gamma \cdot \mu_0 H_{eff}$ [7].

- The **spin-wave free path** $l_{free} = v_{gr} \cdot \tau$ is a distance which SW propagates before its amplitude decreases to its $1/e$ value. The free-path of the long-wavelength BVMSW is usually large and is close to few hundreds of micrometers. For MSSW l_{free} is almost proportional to the film thickness t and, therefore, is much larger in the μm -thick YIG samples. Parasitic loss in the magnetic devices will be inversely proportional to the SW free-path l_{free} .

- General profile of both v_{gr} and, therefore, l_{free} is quite complex, featuring both regions of increase and decline. Nevertheless, the decrease in the wavelength assumes that long free paths are not always necessary. **The ratio** l_{free}/λ , which shows how many wavelengths (i.e., how many unit elements) a wave propagates before it relaxes, is also of importance. The decrease in the wavelength of the exchange waves results in the increase of the ratio l_{free}/λ , that reaches values above 3000 for waves of nanometer wavelength.

- In most practical situations, spin waves are studied in spatially localized samples, such as thin films or strips, which are in-plane magnetized by an external magnetic field. The geometry of a SW waveguide, namely its **thickness** d and its

width w , is a key parameter defining the spin-wave dispersion along with the **saturation magnetization** M_s of the magnetic material, **exchange constant** A_{ex} , and the **applied magnetic field** $\mu_0 H$.

3) *Choosing magnonic materials*: Spin waves are usually studied in thin magnetic films, waveguides or spheres. Choice of the material plays a crucial role in both fundamental and applied magnonics. The main requirements for the perspective magnetic material are: (i) small Gilbert damping parameter in order to ensure long spin-wave lifetime; (ii) large saturation magnetization for high-frequency SW frequencies and velocity; (iii) high Curie temperature to provide thermostability; and (iv) simplicity in the design of magnetic films (and excitation transducers in a form of antennas, if applicable) and in the fabrication processes.

The detailed overview of the most commonly used materials for fundamental magnonics, as well as those with a high potential for magnonic applications, together with their selected spin-wave characteristics is given by Chumak [4]. Among other materials, the author discussed Permalloy (Py), CoFeB and Heusler CMFS compound. Yet, the most promising magnonics material as of now remains a monocrystalline ferrite yttrium iron garnet $Y_3Fe_5O_{12}$ (YIG) grown by high-temperature liquid phase epitaxy (LPE) on a gadolinium gallium garnet (GGG) substrate [100], [101], [102]. This ferrimagnet has the smallest known magnetic loss that results in a spin-wave lifetime of some hundreds of nanoseconds and, therefore, finds widespread use in academic research [103]. The small magnetic losses are due to two main factors: 1) YIG is a magnetic dielectric, hence no free-electron scattering on phonons and minimum (comparing to metals) energy losses via the heat dissipation [102]; 2) the magnetism of YIG is primarily due to Fe^{3+} ions, which have no net orbital angular momentum, causing the spins to be effectively decoupled from the lattice (no spin-orbit coupling, magnetic properties are entirely due to spin and gyromagnetic ratio [7]). Moreover, high quality LPE single-crystal YIG films ensure a small number of inhomogeneities and, thus, suppressed two-magnon scatterings and lower losses [6]. Throughout the majority of its history, high-quality YIG was mainly grown in the micrometer range, which did not allow for the fabrication of YIG nanostructures. Yet, since the development of technologies for the growth of high-quality nm-thick YIG films mere 10 years ago, (e.g., by means of pulsed-laser deposition (PLD) [74], [75], [76], [77], [78], sputtering [79], [78], liquid phase epitaxy [70], [71], [72], [73]), most of the modern nano-magnonics is based on YIG. Although the quality of these films is still slightly worse when compared to micrometer-thick LPE YIG films, it is already good enough to satisfy many requirements of magnonic applications and is still better than the other materials [104].

II. MODERN MAGNONICS: GENERAL OVERVIEW

A. Current state of the magnonic field

The modern field of magnonics is very broad and is growing rapidly every year, involving more and more researchers from

the neighboring fields of spintronics, quantum optics, superconductivity, materials science, and nanotechnology. Probably the most convenient way to present an overview of the direction of magnonics is to refer to the figure by Barman and Gubiotti [105] – see Fig. 4, from the recent field roadmap. One can clearly see that magnonics covers a very wide range of topics, although the majority of the research directions are more fundamental than applied. At the same time, all the basic research studies are aimed at providing new technologies that are attractive for industrial production [14], [105].

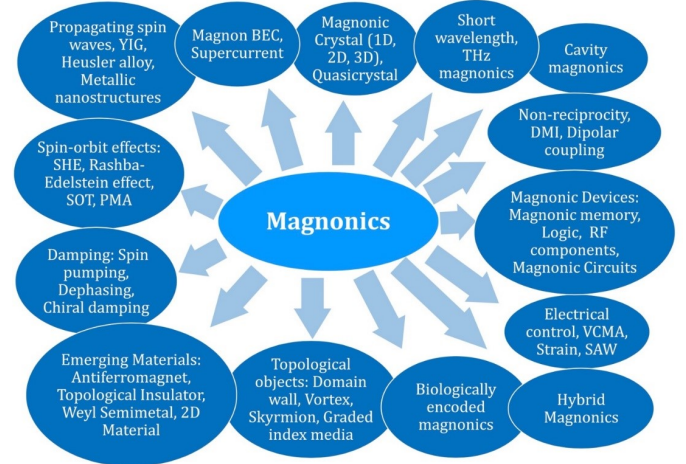


Fig. 4: The many branches of magnonics. Adapted after [105].

B. Vectors of the cutting-edge developments

Indeed, spin waves are already attracting much attention as potential data carriers in novel energy-efficient computing devices or as a storage medium [106], [107], [108]. On the other hand, spin waves in the GHz frequency range are of large interest for applications in telecommunication systems and radars [4]. Since the SW wavelengths are orders of magnitude smaller compared to electromagnetic waves of the same frequency, they allow for the design of micro- and nano-sized devices for analogue data processing [14], [85], [105], [109]. All the aforementioned applied potential, in combination with a rich choice of linear and non-linear properties [9], renders spin waves excellent objects for the studies of fundamental physics as well [4]. One- and two-dimensional soliton formation [110], non-diffractive spin-wave caustic beams [111], wave-front reversals [112], room temperature Bose-Einstein condensation of magnons [113], [114], [115], quantum magnonics [16], [92] and parametric generation of the spin waves in magnonic conduits with circular magnetization precession [116] is just a small selection of examples.

This topic has been partially discussed in [14], [105]. Below, we would like to summarize the most prominent current and expected advances in the magnonics field relevant for the spin-wave based RF devices:

1) *Notable progress in microwave transducers design*: The fundamental method to excite spin waves is by means of an external dynamic magnetic field generated by alternating cur-

rent (AC) in a transducer [104]². The AC current generates an alternating Oersted field via Ampère's law, which in turn exerts a torque on the magnetization in an adjacent ferromagnetic medium. At excitation frequencies above the ferromagnetic resonance, the Oersted field can then excite spin waves in the medium [47]. Direct coupling between the RF magnetic field and the magnetic moments enables rather efficient conversion of electromagnetic energy into spin-wave energy [117]. Energy carried away in SWs propagating perpendicular to the antenna is related to EM energy propagating along the microstrip line by an equivalent radiation resistance [118].

The shape and the dimensions of inductive antennas have a strong impact on the spin-wave transmission. Wide antennas generate a broader wavevector spectrum, enabling the excitation of a wider range of spin-wave modes, which increases the spin-wave bandwidth. However, this comes at the cost of reduced magnetic field strength beneath the antenna. In contrast, narrower antennas produce a stronger, more localized magnetic field, enhancing spin-wave excitation in a specific region. The spacing between antennas must strike a balance: they should be close enough to ensure efficient spin-wave propagation but not so close as to cause cross-talk or interference [119]. As demonstrated by Vanatka et al., [119], a phase-resolved analysis of spin-wave transmission between two antennas with variable spacing enables efficient reconstruction of the spin-wave dispersion relation at room temperature, and potentially in cryogenic conditions. Measurements were conducted on Co-Fe-B and YIG thin films in both in-plane and out-of-plane magnetization geometries for an 11 antenna gap, revealing high resolution in both frequency and k -vector.

Multi-turn (meander) antennas can improve excitation by covering a larger area of the magnetic material. To optimize design parameters, simulation tools like micromagnetic modeling are invaluable for achieving the best performance trade-offs. That is why the efficient antenna's design is detrimental for successful device's functioning. Various novel designs of CPW, ladder and meander antennas have been proposed, and their operational characteristics have been improved [82], [83], [84], [85], [120]. In particular, a lumped circuit model for inductive antenna spin-wave transducers in the vicinity of a ferromagnetic medium was developed [83]. The model considers the antenna's Ohmic resistance, its inductance, as well as the additional inductance due to the excitation of FMR or spin waves in the magnetic medium.

Conventional dipolar antennas suffer from scaling issues and losses due to the near-field interactions with the environment. Alternatively, spin-torque nanooscillators [121], [122] or spin Hall oscillators [123] can be used, but they lack the required bandwidth and spectral purity for computing, while inductive techniques [124], [66] offer broad bandwidth, but are energy-inefficient. Emerging methods like inverse magnetostriction devices [125] show promise but need improvement in energy efficiency. Spin-orbit torques (SOTs), which can rapidly switch magnetization, present an intriguing alternative for spin-wave excitation, as demonstrated by Talmelli et al., [87]. Due to the

specific design of the thin in-plane magnetized Ta/(Co,Fe)B waveguides, the parasitic coupling between the spin-wave emitter and the collector were minimized, and spin-waves with a wavevector up to 6 rad/ μm were excited [87].

Yet, one should always keep in mind that ferromagnet/normal metal system, despite being a standard spintronic model, comes with an enhanced spin-wave damping due to the conductance mixing or spin-torque parameter [126]. The impact of ohmic losses from SW-induced eddy currents in the heavy metal layer on the spin-wave damping in magnetic layer (e.g., single-crystal YIG film) have been experimentally realized by Serha et al., [127], and ways to mitigate the losses have been proposed by Bunaev et al., [128]. The undesired enhancement of Gilbert damping (magnetic losses) can be partially controlled and reduced by positioning a highly conductive metal plate parallel to the structure surface that redirects the eddy currents circulating in the heavy-metal layer [128]. To achieve optimal performance, the capping layer's thickness should be greater than the skin depth of the plate material.

Over the last decade, a significant progress in the design of antennas for various micro- and millimeter-wave applications has been made that allowed to drastically decrease parasitic losses. For example, magnetoelectric-based antenna (piezo-electric–magnetostrictive bilayer) was proposed as a more compact, power-efficient alternative to conventional dipolar antennas due to much shorter wavelengths of utilized acoustic and magnetic waves at microwave frequencies [129], [130]. Applying a microwave signal to such an antenna produces an oscillating magnetic dipolar field, which acts as a source of electromagnetic radiation. The response can be enhanced by acoustic and magnetic resonances. Furthermore, in 2024, Erdelyi et al. [131] presented a computational framework for the design of magnonic transducers aimed to find the optimal geometries that minimize transduction losses. It is qualitatively different from the predecessors as it combines circuit-level models with micromagnetic simulations to simulate complex geometries in the magnonic domain. The model predicted a design of a transducer pair in YIG with 5 dB insertion loss in a 100 MHz band. These rather low losses for micron-scale spin-wave devices were obtained by applying the scaling rules of the antenna radiation resistance to maximize transduction efficiency between the electric and magnetic domains [131]. Further improvement should be addressed during the research and development stage for the specific device.

2) *Advancement in understanding of the nonlinear spin-wave physics:* Nonlinearity refers to a phenomenon where the output of a system is not directly proportional to its input. It arises when interactions depend on the amplitude (intensity) of the input, leading to effects such as frequency shifts, power limitations and wave mixing. In a case of spin waves, nonlinear behavior is observed when the microwave driving power exceeds a certain threshold, causing SW amplitude modulation, manifesting as low-frequency oscillations, self-pulsations or turbulence [117]. On a fundamental scale, this process is driven by the multimagnon scatterings under the momentum and energy conservation laws. If to apply high-power external

²In the description of spin-wave excitation (fundamentals, applications) "antenna" is used interchangeably with "transducer".

oscillating microwave field at twice the frequency of a target mode, it will inject energy into a system to amplify or excite specific SW modes through nonlinear interactions - process known as parametric pumping. It is the only widely used technique for amplifying both linear and nonlinear spin-waves in YIG films in frequencies ranging from a few gigahertz to a few tens of gigahertz, and with maximum gains exceeding 30 dB at room temperature [9].

From the application point of view, rich nonlinear properties of the spin waves can offer signal processing and amplification, logic operations, power limitations or signal-to-noise ratio enhancement. However, up until recently, the very same nonlinearity was rather a limiting factor due to the lack of knowledge in the field. This, for example, did not allow to reach a maximal operational power of the RF devices (especially critical for the power amplifier). Over the years, the magnonics community has accumulated enough knowledge to understand and control SW nonlinearity [9]. For example, efficient nonlinear switching functionality of a directional coupler was recently demonstrated by Wang et al., [10] through the dependency of the output SW intensity of the waveguides on the varying input microwave power. Innovative approach, developed by Chumak et al., [68], used nonlinear four-magnon scattering as an operational principle in the magnonic-crystal based transistor - magnons from the transistor's source are scattered by the localized gate magnons, leading to attenuation before reaching the drain. The strong localization of gate magnons in the magnonic crystal enhances scattering probabilities, amplifying nonlinear effects [68]. Important regarding the operational power of the SW RF devices is the work of Jungfleisch et al. [132], in which the reduction of the YIG film's thickness enables the suppression of parasitic nonlinear multimagnon scattering, which should consequently allow an increase in the operational power.

Nonlinear interaction between two spin-wave signals was investigated by Breitbach et al., [133] in a Ga:YIG film. Demonstrated results showcase an all-magnonic erasing process, offering potential for complex logic and neuromorphic functionalities [133]. Nonlinear phenomena also offer new approaches to signal processing using combined microwave/spin-wave devices, as demonstrated by Serga et al., [134] in their study of parametrically stimulated recovery of a microwave signal. It was shown that MW signals carried by dipolar spin waves in a tangentially magnetized magnetic film can be stored as standing dipole-exchange modes and recovered using a double-frequency parametric pumping mechanism.

3) *Nanoscaling*: Smaller, faster, more efficient – is a motto for technological progress that led to the computerization and automatization of everyday life. Applied magnonics for a long time was able to address only the last two requirements due to the fabrication challenges of its most prominent and promising material – YIG. Nevertheless, recent success in the fabrication of high-quality thin YIG structures became possible with the advancements in nm-thick liquid phase epitaxy technology [72], [73]. The achieved thickness of LPE-grown ultrathin films was as small as 9 nm, while the lateral sizes of the YIG structures were minimized down to 50 nm.

Advanced nanoscale spin-wave networks for applications in neuromorphic computing, stochastic and reservoir computing, and quantum computing were extensively reviewed by Wang et al., [135], highlighting transformative possibilities for next-generation computing paradigms. Alternative direction of 2D low-dimensional Van der Waals structures is at the beginning of its intensive growth and will lead to the next step of miniaturization of magnonic devices.

4) *Micromagnetic simulation tools for spin-wave dynamics*: Over the past few decades, the growing complexity of fundamental physical investigations and advancements in magnetic systems has increased the demand for powerful micromagnetic simulation tools. A key tool in magnonics is the micromagnetic semiclassical theory, where magnetization is represented by a continuous unit-vector field, and interactions are described by nonlinear partial differential equations [14]. This theory allows the resolution of domain walls and spin waves without considering individual atomistic moments, though analytical solutions are often not feasible. To bridge the gap between real systems and simulations, numerical methods such as the finite-difference and finite-element methods are used to solve micromagnetic equations [136], [137], [138]. To reduce the complexity and computational costs, modern tools rely on parallel computing architectures like GPUs [139], [140], [141] or novel algorithms, such as machine learning [135].

Micromagnetics in the frequency space is preferred in magnonics due to its efficiency compared to time-domain simulations. This approach relies on the linearization of the Landau-Lifshitz-Gilbert equation providing dynamic modes and power-spectral densities, and has recently been extended to include nonlinear effects, making it a powerful tool for designing magnonic devices [142], [143], [144]. Additionally, magnonic devices often integrate spintronics effects, such as spin pumping and the inverse spin-Hall effect, requiring modifications to the simulations. A self-consistent coupling of micromagnetics with spin-diffusion models has been discussed in [14], incorporating various spintronics effects. While macroscopic systems can be predicted to some degree, simulating entire devices remains challenging. For designs with few variables, simple algorithms like binary search algorithms with a fast forward solver can be effective, as demonstrated by Wang et al., [98], but for more complex, high-dimensional designs, advanced optimization methods, such as gradient-based algorithms, are necessary.

Many of the excellent available simulation tools are open-source and user-friendly, e.g., Magnum [145], mumax [146], TetraX [147], Boris Computational Spintronics [148], NeuralMag[149] and OOMMF [150].

5) *Machine learning and inverse design*: Revolutionary approach of the inverse design, in which any functionality can be specified first, and a feedback-based computational algorithm is used to obtain the device design, was recently introduced to magnonics. This methodology, as shown by Wang et al., [98] allows to optimize the device design, simultaneously saving the fabrication and time-resources. The universality of this approach was demonstrated with a proof-of-concept [98] based on a ferromagnetic slab, patterned in a way to explore

linear, nonlinear and nonreciprocal magnonic functionalities, and create magnonic (de-)multiplexer, a nonlinear switch and a circulator. Inverse design was also used by Papp et al., [13] to explore a neural network hardware, where all neuromorphic computing functions, including signal routing and nonlinear activation, are performed by spin-wave propagation and interference. Weights and interconnections of the network were realized by a magnetic-field pattern that is applied on the SW propagating substrate and scatters the spin waves.

Kiechle et al., [151] further used the capabilities of machine-learning algorithm to create a spin-wave lens - device aimed at precise spin waves focus. The design was verified in the *mumax*³ micromagnetic solver and experimentally implemented by creating effective magnetization landscapes in 69 nm-thick YIG film via the focused-ion-beam irradiation. The proof-of-concept demonstrates a pathway for developing advanced spin-wave devices, such as SW processors or neuromorphic systems.

A milestone achievement in the inverse-design methodology was demonstrated by Zenbaa et al., [99] that developed a versatile reconfigurable magnonic inverse-design device with 10^{87} degrees of freedom, enabling a wide range of functionalities. Two optimization algorithms were employed to tailor the device for linear RF communications, 5G and 6G technologies, as well as to achieve nonlinear functionalities for logic gates, reservoir computing, and neuromorphic computing. In particular, RF notch filter with a 5 MHz bandwidth for any center frequency (achieving up to 48 dB signal suppression) and an RF demultiplexer were realized on the same device. The signal modulation was achieved over the four orders of magnitude, showcasing its exceptional performance [99]. One of the main drawbacks of inverse design, namely the limitation of computing systems memory required for numerical simulations of complex devices, can be addressed by using the adjoint method, as discussed by Voronov et al., in a recently submitted paper [152].

Hence, despite its infancy, the topic of inverse design magnonics has found wide support and interest from the community, as it opens new perspectives for applied magnonics. In particular, we believe that the same approaches can be used to solve or mitigate all of the major obstacles to spin-wave RF devices discussed below, including parasitic losses and limited operating powers.

6) *Non-reciprocity of spin waves*: Future progress in communication systems relies heavily on the miniaturization and integrability of non-reciprocal RF components such as circulators, isolators and directional couplers [153]. The landmark performances of ferrite technology [35], which is based on the classical non-reciprocal propagation of EM waves in gyrotropic bulk media (will be briefly discussed in *Section III* of this Review), are yet to be replaced with scalable solutions for ICT - an issue which micro- and nanoscaled magnonics can address.

Spin-wave non-reciprocity is a phenomenon, which refers to the asymmetrical propagation of spin waves in opposite directions within a magnetic material (different frequencies for $+k$ and $-k$). Amplitude non-reciprocity is an inherent

property of surface spin-wave modes [154], and it can be further engineered through various coupling mechanism such as: (1) combination of broken inversion symmetry with the spin-orbit interaction leading to the chiral Dzyaloshinskii-Moriya interactions [155], (2) mean curvature of nanotubes in combination with the dipole interaction observed in magnetic nanostructures [156], or (3) dipolar interactions in multilayers [157], [158], [159].

In recent years, an intensive on-going research is dedicated to the nonreciprocal magnonics. The ability to inhibit signal flow in one direction while allowing it in the reverse direction plays a crucial role in either protecting microwave devices from reflections, isolating the transmitter from the receiver in radar architecture, or shielding qubits from their environment.

7) *Quantum magnonics*: This leading spin-wave research area is focused on single magnons and their quantum properties, such as entanglement, hybrid system coupling and Bose-Einstein condensation among others. Integration of classical magnonic computing concepts with quantum sensing or computing on a single nanoscale platform has recently garnered significant interest [135]. The field's emergence less than a decade ago was heavily influenced by Lachance-Quirion et al., [90] work on superconducting qubit entangled with ferrimagnetic crystal in a 3D microwave cavity. This work paved the way for high-efficiency single-magnon detectors vital for sensing and hybrid quantum systems, but was focused on confined non-propagating FMR modes in YIG spheres. The next critical milestone, predicted by Wang et al., [135], is the excitation and detection of propagating single magnons, which is essential for quantum information transport and processing.

To facilitate the quantum magnonics, it is crucial to accurately predict the behavior of a magnetic system in cryogenic environment (typically YIG films grown on GGG substrate). Serha et al., [160] revealed that an inhomogeneous stray magnetic field, produced by the partially magnetized GGG, strongly influences the FMR frequency shift (which is a case only in mK temperatures). The investigation of the spin-wave damping at millikelvin temperatures versus wavenumber was made by Shmoll et al., [161]. First experimental study of a propagating spin-wave in a 100 nm-thick YIG from room temperature down to 45 mK was presented by Knauer et al., [92]. Microstrip nanoantennas were used for electrical excitation and detection of spin waves with clear transmission characteristics over a 10 μm distance. Smart experiment planning helped to minimize the strong impact of GGG and proved that large-scale integrated YIG nanocircuits remain feasible for future applications. A key limitation of quantum magnonics is its reliance on low temperatures to suppress thermal magnons (10^{18} cm^{-3} at equilibrium with the phononic bath of a solid). That said, quantum magnonics develops fast and offers transformative potential for sensing, information processing, and hybrid quantum technologies.

8) *Alternative materials*: Material's choice is decisive for the magnonic device functionality. To operate with waves of maximized speed in structures at the industry-competitive nanoscale, materials with large spin-wave exchange stiffness λ_{ex} are mandatory. In addition, the fast exchange-dominated

spin waves (rather than MSW) would not only allow for the operations with microscaled antennas, but would also give the freedom required for the engineering of data-processing units, since the exchange-dominated dispersion relation is highly isotropic. In this context, it is promising to study **ferrimagnetic insulators which are close to the magnetic compensation**, since low saturation magnetization M_s tends to increase λ_{ex} . A good example would be Ga-substituted YIG. Studies of LPE-grown partially substituted nm-thick Ga:YIG films [162], [163] with a decreased M_s and a strong stress-induced out-of-plane uniaxial anisotropy demonstrated that the exchange stiffness in Ga:YIG film is about three times larger than the one for pure YIG. That, consequently, leads to much higher group velocities and isotropic spin waves. Thus, Ga:YIG might enable the operation with fast and isotropic spin waves in future magnonic networks.

Hexaferrite is another promising candidate for the high-frequency applications (high band of 5G/6G). This class of ferrites is known for the high operating frequencies > 50 GHz and low losses in a wide frequency range [35]. Therefore, many non-reciprocal RF applications (circulators [164], isolators [165]) and magnetostatic devices (filters [166], resonators [167]) could be fabricated based on hexaferrites. A typical representative of this class, pure BaM ($BaFe_{12}O_{19}$ - M-type barium hexaferrite), allows for the operations with frequencies up to 60 GHz for moderate magnetic fields of < 1 T [168]. The total loss in RF devices is influenced by relaxation parameters, such as the Gilbert damping parameter α , which together with the SW frequency, f , determines the lifetime of the spin wave. In hexaferrites, the already achieved values of $\alpha \sim 7 \cdot 10^{-4}$ [169] are significantly better than in the majority of magnetic metals, despite the low structural quality in the investigated PLD-grown samples.

III. SPIN-WAVE TECHNOLOGY FOR RF APPLICATIONS

The emergence of 5G and the progression toward 6G technologies have renewed focus on microwave communication devices. Key components, including filters, frequency-selective limiters, amplifiers, delay lines, mixers, modulators, and frequency synthesizers, require adaptation to meet the demands of new frequency bands and communication protocols. Magnonics can help to address some of the challenges due to unique combination of functionalities, unavailable in conventional RF electronics or in SAW-based devices, - reconfigurability, scalability down to sub-100-nm sizes, a wide operational frequency range from sub 1 GHz up to THz, and nonlinearity (more details on advantages in *Chapter IV*).

Moreover, the spin-wave frequency, wavelength, wave group velocity, and attenuation can be tuned within limits by varying the magnitude of the bias magnetic field [42]. The degree and efficiency of such tunability depend on the choice of magnetic material. Ideal microwave materials possess high magnetization, high permeability, high permittivity, high electrical resistivity, and low electrical and magnetic losses. Insulating magnetic materials that fit this criterion include ferrites and related magnetic oxides [35]. The realization of the majority of the microwave devices and concepts is based on YIG

films (as films provide greater uniformity than bulk crystals). SW propagation efficiency is directly related to crystal quality: microwave losses are usually proportional to the FMR linewidth, with low losses corresponding to small values of linewidth [42]. Therefore, YIG with the narrowest FMR linewidth is a primary material in SW-based applications. In terms of magnetostatic waves, YIG demonstrated relatively low propagation losses of around 20 dB/ μ s at 9 GHz [40]. By comparison, propagation losses for SAW devices on lithium niobate are more than 100 dB/ μ s at 9 GHz [42]. MSW devices allow for the wide frequency tuning, with a bandwidth roughly proportional to the saturation magnetization of the ferrimagnetic film. The ideal bandwidths of devices based on YIG films is around 2 GHz [40], with further factors, such as film's dimensions and antennas efficiency contributing to the real value. Over this bandwidth the wavelength of the SW can change from mm to angstroms. Thus, useful time-delay characteristics were usually limited to bandwidths of around 1 GHz [40]. In addition to these unique dispersive and tunable features, MSW are readily launched by simple transducer structures [40].

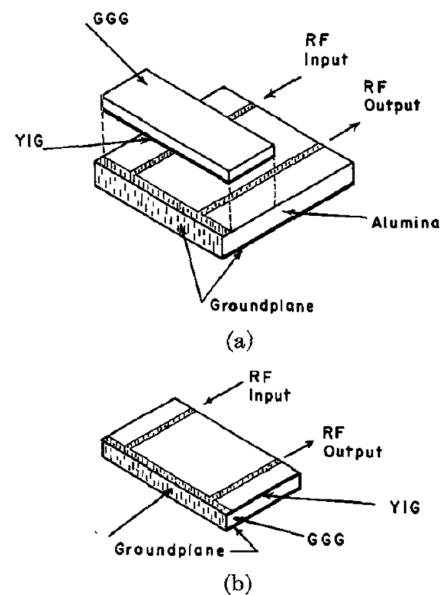


Fig. 5: Microstrip excitation of magnetostatic SWs a) with a standard alumina substrate; b) with a GGG substrate. Adapted after [118]

On a macroscale, convenient excitation of spin waves could be realized by a simple microstrip antenna - metallic patch on a dielectric substrate with a ground plane underneath (Fig. 5). Because coupling from electromagnetic to spin waves and then back to electromagnetic signal is rather strong, a single metallic strip is sufficient for mm-sized devices (more on the transducers and antennas in *Section II*). This is in contrast to SAW excitation, where a meander-type interdigital transducer is necessary [118]. Experimental investigations of the microstrip spin-wave excitation in millimeter-sized, micrometer-thick YIG samples (Fig. 5) revealed the following trends [118]: (i) at a fixed bias field and specific microstrip geometry, the excitation bandwidth increases approximately proportionally to the YIG film thickness and saturation magnetization; (ii)

radiation resistance shows only a slight dependence on sample thickness; (iii) for a given geometry, the excitation bandwidth narrows as the bias field increases, while the maximum radiation resistance value rises. Consequently, for optimal wideband excitation, the microstrip width should be reduced to a value comparable to the film thickness, simultaneously ensuring proper impedance matching and minimal ohmic losses. However, for the modern microscale devices, electromagnetic waveguides tend to become highly resistive, with significant ohmic losses that can hinder efficient signal transduction due to increased insertion loss [131]. This limits the commercial applications, indicating a strong need for IDT design optimization. This challenge has currently spurred extensive research, and was briefly discussed above in the *Section II*.

In terms of applications, concepts of RF devices have been proposed, including filters (e.g., based on magnonic crystals), delay lines, phase shifters, frequency separators, Y-circulators and isolators, phase and amplitude multiplexers, receivers, spectrum analyzers, power limiters, signal-to-noise enhancers, and wave-front reversers [109].

It is important to distinguish between two conceptually different approaches to the realization of SW RF applications:

1) In one case, RF devices are based on keeping the signal (energy) within the electromagnetic wave, and only for some frequencies the energy is absorbed or re-emitted by the magnetization precession in magnetic spheres of thin films [35], [88], [89], [170], [171], [172]. These devices operate with ferromagnetic resonance (wavenumber $k = 0$) or standing spin wave modes, and are well-suited for stopband filters, specially designed passband filters, resonators, microwave sources. The delay line is difficult to achieve with this approach because the information is transmitted with a speed of light. In contrast, these devices offer very low insertion losses, which in fact should be the same as for commonly used microstrip line-based non-magnetic microwave engineering (more than 30 dB isolation and less than 0.1 dB of insertion loss [35]).

2) Another approach to SW RF applications is based on the excitation of propagating spin waves by an RF field applied to a spin-wave transducer and their subsequent detection by another transducer. This approach is more similar to the commonly used SAW-based technology and is highly suitable for the realization of delay lines, since the delay is defined by the spin wave velocity, which can be easily tuned by a variety of parameters [40], [42], [45], [173]. The main drawback of such an approach is that the insertion loss is given by the efficiency of the conversion from electromagnetic to spin wave by the input transducer, by the loss of the spin waves while propagating between the transducers, and by the efficiency of the back-conversion from the spin wave to electromagnetic wave. Nevertheless, the simple analysis of the 2.5 dB insertion loss in [45] shows that the efficiency of the conversion can reach $> 80\%$: -2.5 dB means 0.562 in power ratio, hence using the rough estimation that the losses are the same for conversion, detection and spin wave attenuation, we get $\sqrt[3]{0.562} = 82.5\%$ as the ratio for the spin wave transducer efficiency. Further improvement of this value would make the

SW RF devices compelling considering the wide frequency range, scalability and other advantages discussed below.

The first peak of interest from both scientific and industrial communities was in 60s-80s, as seen in historical outline. A considerable part of the articles even then was dedicated to the data transmission systems, where MSWs were proposed as complementary to SAWs for the microwave signal processing [118]. In addition to a relatively low propagation loss and ease of excitation, SWs' useful frequency range begins where that of SAW leaves off, i.e., at 3 GHz [118]. Because SWs are slower than EM waves by two to four orders of magnitude, compact devices can be built with the linewidths in the 10-500 μm -range, allowing simple processing techniques [42]. This huge difference compared to EM waves was a reason why dipolar SWs were often called magnetostatic. Magnetostatic spin waves have a potentially wide application field [40]. Historically, a lot of attention was given to broadband microwave receivers (frequency channelizers, filters, dispersive delay lines for compressive receivers, delay lines for pulse storage, and frequency selective limiters, etc.), and to beam steering of phased array antennas by variable time delay [40].

Most comprehensive summary of the industry-oriented SW-based microwave devices was given in the special issue of *Proceedings of the IEEE*, 76(2) from February 1988 (all the information below was taken from the different subsections of this issue, all rights for the text and figures belong to the rightful authors). In most cases, experimentalists discovered effects and made devices at a rate far outpacing the theoreticians' ability to interpret, much less predict, performance [43]. With today's knowledge and advancements in the field, we can improve older designs, adjusting them to the modern demands of science and industry. In the following text, a brief overview of selected SW devices is discussed - their role, current technology and up-to-date SW analogues.

A. SW filters

RF filters are essential components in communication systems designed to control the flow of signals by allowing certain frequencies to pass while blocking others. By selectively filtering frequencies, RF filters help prevent interference, improve signal clarity, and ensure that only the desired signals reach specific parts of the system. They are critical for a wide range of applications, including telecommunications, broadcasting, and wireless communication, where managing and isolating specific frequency bands is essential for efficient operation.

For years, high-performance passive RF filters have predominantly relied on silver-coated ceramic monoblock structures, offering an optimal balance between attenuation, insertion loss, and compactness. Advances in material science have improved these ceramics by reducing dielectric losses $\tan \delta$, and increasing the dielectric constant ϵ_r , which has allowed for significant size reductions. However, their bulkiness (typically in the millimeter range) remains a major limitation for integration with compact mobile devices that require microscale RF technology. Efforts to further miniaturize RF devices by combining ceramic dielectrics with magnetic materials and optimizing

structures have shown promise but introduce manufacturing challenges and risk performance degradation. Moreover, the primary performance bottleneck has shifted from dielectric loss to conductor loss in the silver coating, signaling a need for alternative solutions.

Surface acoustic waves technology allowed to address some of the limitations of the conventional filters [1], [2] leading to modern multi-band, multi-standard mobile communication systems. The SAW filters market is extensively evolving, including such tech giants as Abracon, API Technologies, Kyocera, Microchip Technologies, Murata Manufacturing, Qorvo, Qualcomm Technologies, etc. The key advantage of surface acoustic waves is a significantly lower group velocity compared to electromagnetic waves, allowing bulky RF devices (due to their centimeter-to-meter wavelengths) to be miniaturized by a factor of 100,000. This enables compact, chip-based signal processing solutions for mobile communications within the RF range of tens of megahertz to several gigahertz. Nevertheless, the high-frequency (e.g., 5G high-band @26 GHz) limitations still persist [3], as SAW suffers from significantly increased damping, with insertion losses around 40 dB at 15 GHz [174] as well as the exposure limitations of interdigitate transducers (IDTs)[1], [3].

BAW filters have smaller losses at higher frequencies (above ≈ 3 GHz) comparing to SAW-based ones due to their superior resonator Q-factor [1]. Novel technologies like Temperature Compensated SAW (TCSAW) and piezoelectric-layer-based filters may shift the balance back in favor of SAW technology, yet it is still uncertain whether SAW filters will successfully extend their reach beyond the 3 GHz frequency range. Conversely, BAW-based RF filters are already available for mid-range frequencies (up to 6 GHz); however, the high-frequency range (30 GHz) is still largely unexplored. Currently, the main impediments are increased damping and inefficient energy transfer between the transducer and the acoustic wave within the propagation medium at higher frequencies, strict requirements for BAW isolation from the substrate to prevent unwanted energy dissipation, and the subsequent complexity of the fabrication process [3].

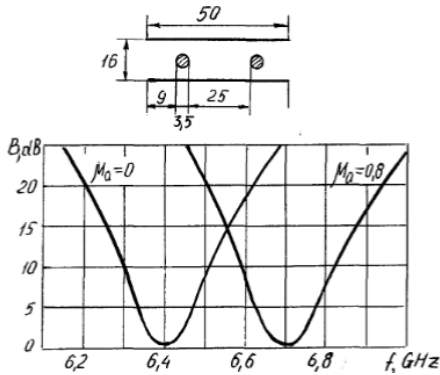


Fig. 6: Two-order ferrite filter response. Adapted after [175].

Magnonics offer superior operational frequency region and technological flexibility. Because the bandwidth of SW delay lines can be controlled by varying the transducer dimensions and the YIG/ground plane separation, these devices can be

used in tunable filter applications [42]. SW narrow-band filters with bandwidths down to 30 MHz at microwave frequencies have already been demonstrated [176]. Furthermore, when the transducers are separated from the YIG film via a spacer layer, even narrower bands can be obtained. Such a filter was tuned over the 3-7 GHz range with less than 0.1 dB peak-to-peak amplitude ripple [42]. By careful adjustment of the transducer width, the YIG film thickness and by minimizing the coupling to width modes, wide-band FVMSW filters with more than 45 dB of out-of-band rejection in the operational range from 0.3 to 12 GHz were obtained [177].

The tunable microwave filter for mobile communications systems was also proposed in 1990 by Kapilevich and Safonov [175]. A device is based on polycrystalline YIG-ferrites resonators in the form of cylinders, which are placed in the center of the waveguide. Application of the polycrystalline materials enables the increase of the microwave power passing through the filter by three orders. None of the non-linear phenomena were experimentally detected while applying continuous power up to 2 W. As a result, the same filter can be theoretically used both in the receiving and transmitting channels of the radio-relay equipment. The range of such a waveguide-ferrite resonator's frequency is mainly tuned via the diameter of the ferrite cylinders. Many different designs were developed and measured with an exemplary two-order filter presented in Fig. 6.

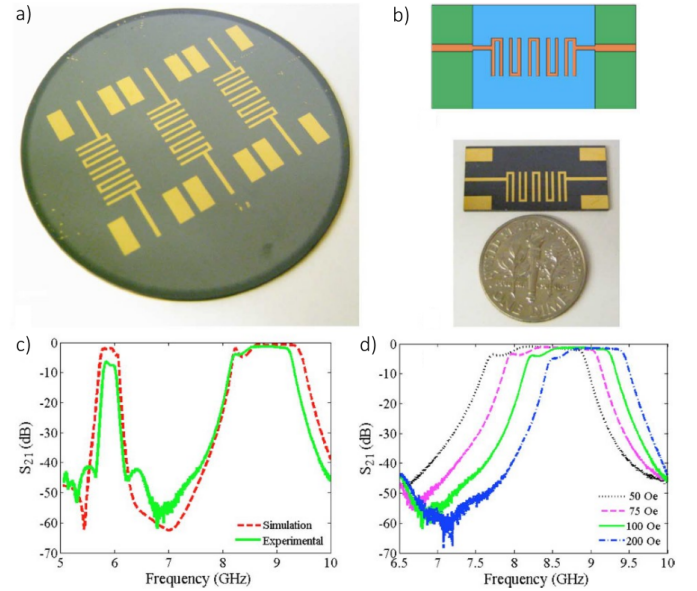


Fig. 7: (a) Photograph of patterned 50 mm diameter YIG wafer. (b) Design and photograph of fabricated bandpass filter device. (c) Simulated and measured passband characteristics of the ferrite microstrip hairpin line coupled resonator bandpass filter. Measured spectrum is collected under applied magnetic field of 10 mT. (d) Passband characteristics of the ferrite microstrip hairpin line coupled resonator bandpass filter under applied magnetic field from 5 to 20 mT. Adapted after [170].

The device consists of the YIG ferrite cylinders of 3.5 mm diameter each, placed 25 mm apart from each other and 9 mm from the input cross-section. The frequency tuning was measured to be 300 MHz under 20 kA/m bias magnetic field.

The losses in the bandpass were 0.5 dB, and the Voltage Standing Wave Ratio (VSWR) was 1.5. The theory on magnetodynamical free and forced oscillations in ferrite spheres of larger size (the dimensions are not small in comparison with the length of electromagnetic wave in the substance of the sample) is different from the conventional case [6], and was comprehensively provided by Melkov in 1974 in the *Journal of Radio Engineering and Electronics*.

Since 2010s, interest to the MW filter was renewed. Among the first new-wave designs was a bandpass filter with excellent characteristic by Gillette et al., [35], [170]. The proposed device consists of a 5-pole Chebyshev bandpass filter implemented in microstrip hairpin-line coupled resonator geometry on a polycrystalline YIG substrate, biased and tuned with an external bias field above the FMR frequency (Fig. 7). The dynamic tuning of the proposed device is realized by varying the magnetic permeability of the substrate via the applied magnetic field. Operation sufficiently far from both resonance conditions is necessary to obtain a low-loss performance [35].

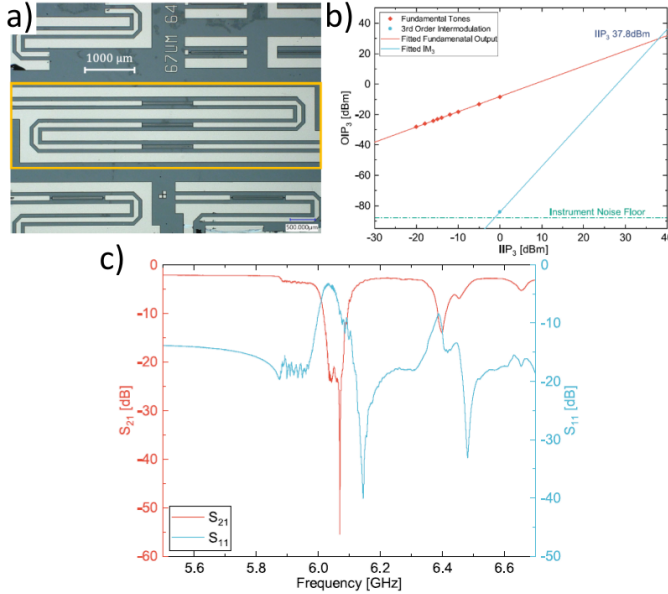


Fig. 8: (a) Optical image of fabricated third-order filter (yellow box). Three YIG resonators have slightly different widths $W_1 = 73 \mu\text{m}$, $W_2 = 70 \mu\text{m}$, and $W_3 = 67 \mu\text{m}$. (b) Measurement of the passband IIP3. The IIP3 point is estimated to be over 37.8 dBm. (c) Measured S parameters of the third-order YIG bandstop filter with a 390 mT bias center frequency of the stopband is 6.07 GHz. Adapted from [89].

Latest achievement in the field of MW filters was done by Feng et al., [89] that successfully designed, fabricated, and characterized a planar monolithic YIG Chebyshev bandstop filter (Fig. 8) via the micromachining technology. The device has a tunable frequency, low insertion loss, and high rejection. Under 390 mT bias out-of-plane magnetic field, the bandstop filter showed 55-dB maximum stopband rejection at a center frequency of 6 GHz, with 2-3 dB passband insertion loss and 37.8 dBm passband IIP3 (Third order Input Intercept Point). By applying different bias fields, the stopband center frequency was tuned from 4 to 8 GHz while maintaining more than 30-dB rejection. Incorporated with proper design

of tunable compact electromagnet, this new filter can provide attenuation of spurs appearing across the 5G [89].

One of the best MSSW-based filter parameters in terms of insertion loss were shown by Bobkov et al., in 2002, Fig. 9 [45]. Authors demonstrated filters based on a metal dielectric-ferrite (MDF) structure with an acute angle between the wave propagation direction and a bias magnetic field (Fig. 9(a)). Transducer antenna for generation and detection of MSSW is designed in a shape of a microstrip line and is based on the dielectric substrate with a high permittivity (e.g., $D_k \sim 10$). The surface of the dielectric substrate is coated with a ferrite layer. In such a device, the bandwidth adjustment, regardless of other parameters, became possible. Moreover, presented approach can also allow for the independent center frequency tuning and the bandwidth adjustment of each channel in multi-channel filters. **The attainable insertion losses and out-of-band rejection in such a SW filter were less than 2.5 dB and more than 40 dB, respectively (Fig. 10(a)).**

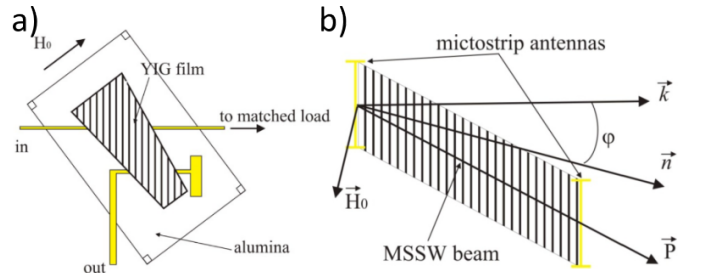


Fig. 9: (a) Magnetostatic spin wave filter tuning. (b) Explanation of the MSSW MFD filter working principles. Adapted from [34], [45]

The authors further elaborated on this approach in the respective chapter of a fundamental magnonics book „*Yttrium: Compounds, Production, and Applications*”[34]. Zavislyak and Popov justified the MSSW as the best spin-wave mode to realize the efficient MW signal processing with an associated single-mode spectrum, nonreciprocity and high efficiency of excitation by simple transducer structures. These advantages were capitalized upon in the developed prototypes of MSSW MDF band-pass filters and filter banks [34], see Fig. 10.

Similarly to the concept presented in Fig. 9(b), a core operating principle of the proposed filters is based upon a fact that MSSW wavevector \vec{k} is oriented in the structure plane at an arbitrary angle φ to vector \vec{n} , and is dictated by the transducer's structure. \vec{n} = vector, orthogonal to H_0 , \vec{P} = MSSW beam. As the angle φ within the $\pi/2 < \varphi \leq \pi$ area becomes narrower, the frequency range of such MSSW decreases as well, enabling an efficient control of a variable-passband filter. The microstrip transducer used for MSSW generation and reception are located on the dielectric layer surface adjacent to the ferrite layer [34]. Thus, the MSSW located at the ferrite-dielectric interface are excited most effectively. Simultaneously, the MSSW spectrum can be shifted in frequency by changing the magnetization field value. The magnetic field intensity H_0 is controlled by a magnetic shunt made of magnetically soft material, and the magnetization field is provided by a small samarium cobalt magnet above the metal screen of a microstrip line. By varying the distance

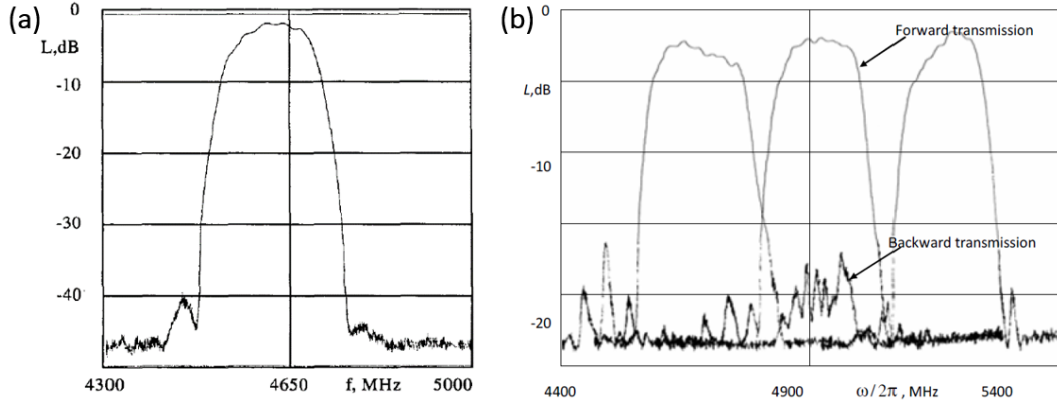


Fig. 10: (a) Insertion loss of the YIG-based μm -thick spin-wave filter. (b) 16-channel MSSW filter bank's amplitude frequency characteristic. Adopted from [34], [45].

between the magnet and the shunt from 0 to 3 mm, one can change H_0 within 80-140 mT range, leading to about 4-6 GHz variations in the central frequency of the filter passband.

The important characteristic of the considered prototype is a non-reciprocity, i.e., a high attenuation factor when the signal is transmitted from the output to input (at reverse connection) [34]. Thus, it performs simultaneously the filtering and isolating function. Fig. 10(b) also shows the respective amplitude frequency response at the reverse connection for the middle bandwidth. The attenuation in this operational mode is at least 34 dB, which may be very useful in practical

applications of the filter. Based on the same principles, a 16-channel filter bank was developed. The device operates in the range of 4-6 GHz, with channel bandwidths 125 ± 5 MHz overlapping at the level of -3 dB, and allows for independent control both of the central frequency and bandwidth of each channel. The insertion loss in either of channels does not exceed 11 dB, which further may be reduced to 8 dB [34].

Among the lowest losses achieved so far were those, presented by Wu et al., [178] in their nonreciprocal tunable bandpass filters with ultra-wideband isolation based on magnetostatic surface spin waves. MSW were excited in a YIG

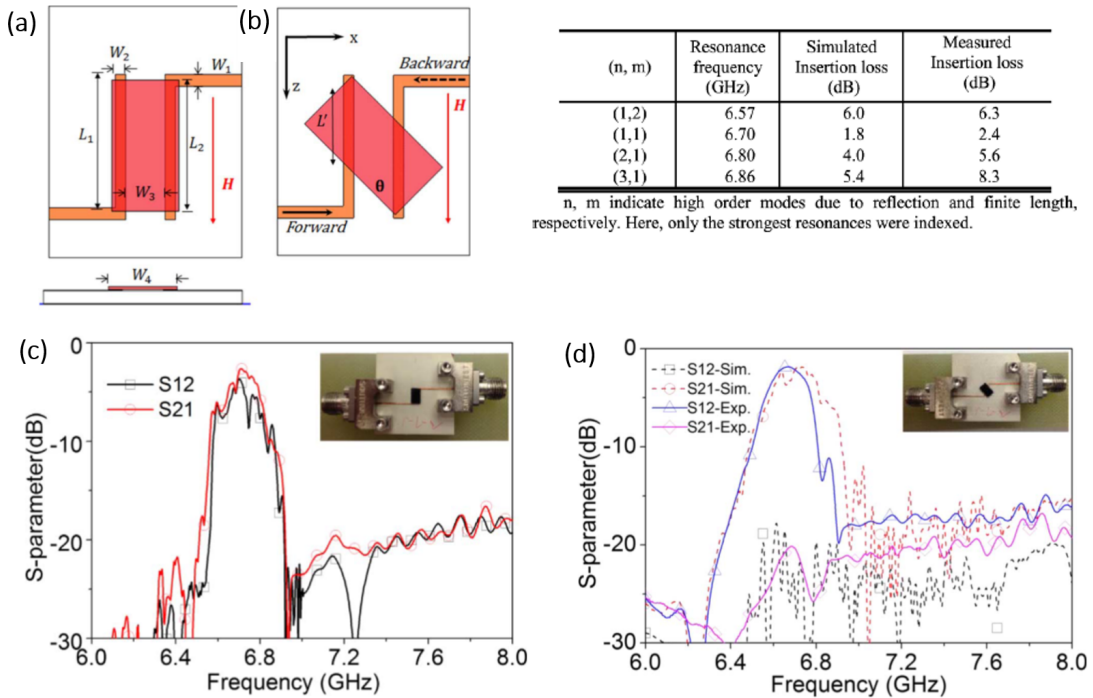


Fig. 11: Geometry of the proposed bandpass filters. (a) Inverted-L-shaped microstrip transducers with parallel YIG slab alignment. (b) Inverted-L-shaped transducer with rotated YIG slab of μm -range thickness. $W_1 = 0.37$ mm, $W_2 = 0.32$ mm, $W_3 = 1.2$ mm, $W_4 = 2$ mm, $L_1 = 4$ mm, $L_2 = 3.6$ mm, $L' = 2.6$ mm and $\theta = 45^\circ$. Table: indexing of resonance modes. (c) Measured results of bandpass filter with YIG resonator aligned parallel to the transducer, according to (a) scheme, under DC magnetic field of 1.6 kOe applied perpendicular to the feed line. (d) Simulated and measured results of bandpass filter with a YIG resonator aligned 45° against the transducer, as shown in (b) scheme. Adapted from [178].

slab loaded on an inverted-L-shaped microstrip transducer pair, as shown in the Fig. 11(a,b). Simulations of the S_{21} and S_{12} responses were reciprocal, with a predicted insertion loss around 1.8 dB at the primary resonant frequency of 6.7 GHz, and the 3 dB bandwidth of 170 MHz. However, measurements of the parallel configuration (Fig. 11(a)) showed higher than predicted insertion loss of around 2.4 dB (Fig. 11(c)) due to roughness of the edges from the fabrication process (Fig. 11 – Table). The rotation of the YIG film leads to the nonreciprocal performance and the elimination of the standing-wave modes, leading to the slab width affecting the propagation losses rather than the resonant frequency. Also, the passband becomes much smoother due to the suppression of the reflections from the edges. The insertion loss of forward transmission is about 1.65 dB at 6.7 GHz, with a bandwidth of 220 MHz (3.2 %), while the reverse transmission has isolation greater than 22 dB (Fig. 11(d)). In general, the tunable resonant frequency of 5.2–7.5 GHz of a bandpass filter was obtained by the authors [178] under the bias field of 1.1–1.9 kOe applied perpendicularly to the feed line. Power-handling capability of over 30 dBm has been achieved at room temperature. The demonstrated passband filter is promising in C-band RF front-end and other microwave circuits.

Basically any magnonic crystal can serve as a microwave filter (band-pass, band-stop) [58], [56], [62], [42] due to their ability to tune the spin-wave transmission characteristics (bandwidth, stopband, passband) via the tailoring of its periodic structure parameters. Additionally, as mentioned in the *Milestone history section*, magnonic crystals are strong candidates for other passive RF devices, such as resonators [179], [180], phase shifters [181], delay lines [182], and other multi-magnon devices [183], making them highly versatile in spintronic and magnonic applications.

B. SW channelizer

A channelized receiver (also regarded as channelize receiver/ multichannel filterbank) is a sophisticated architecture that divides the input signal into separate frequency bands,

enabling simultaneous monitoring, filtering, and analysis of multiple channels, which is essential for applications in telecommunications, radar, and electronic warfare. SW channelizer offers small size, operation at microwave frequencies, and higher dynamic range than Bragg cells or compressive receivers [40] (Fig. 12). If to follow a naive design of a filterbank as a simple array of filters, a rather complex, large and expensive system structure would be required to cover the expected frequency range. Therefore, for practical reasons, a typical SW device consists of a single filterbank with a bandwidth of 1–2 GHz, and wide RF coverage is obtained by "folding" multiple frequency ranges into the bandwidth of the filterbank. Resulting frequency ambiguity can be avoided by using broad-band auxiliary detectors within each band. Alternatively, the filterbank can be "time-shared" among the frequency bands. YIG-based MSW filterbank [40] consisted of 13 narrow-band delay lines arranged along an input manifold. Each delay line consists of a strip of LPE-grown YIG/GGG film, 1-mm wide and approximately 12- μ m thick. A magnetic bias field was applied normal to the YIG film surface to excite FVMSW. Narrow-band characteristics (Fig. 12(a)) were obtained by 0.5 mm wide transducers spaced 160 μ m from the YIG film and by use of reflecting ends on the YIG film. The distance between the reflecting end of the YIG film and the transducer was adjusted to provide constructive interference between the reflected and direct waves at the channel-center frequency and destructive interference on the upper passband skirt and the center of the first sidelobe. The channels are uniformly spaced in frequency with a channel-center frequency loss of 21 ± 1 dB. All of the channels show an out-of-band rejection of 50 dB or greater [40].

C. SW phase shifters

RF phase shifters are critical components in radio frequency (RF) systems, designed to manipulate the phase of an electromagnetic signal while preserving its amplitude. They play a key role in applications such as phased-array antennas, radar systems, and wireless communication, where precise control

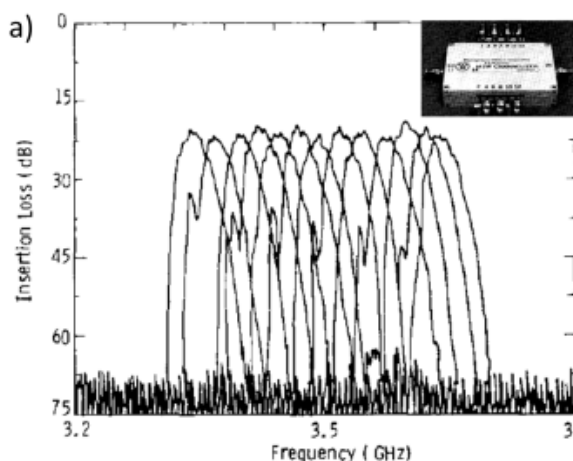


Table 1 MSW Filterbank Performance

Parameter	Current	Projected
Bandwidth	260 MHz	few GHz
Channel bandwidth (3 dB)	20 ± 2 MHz	10–50 MHz
Center frequency	3425 MHz	2–18 GHz
Number of channels	13	20–100
Insertion loss	21 ± 1 dB	< 15 dB
Single tone dynamic range	68 dB	75 dB
Two tone dynamic range	> 50 dB	70 dB
Channel volume density	3.6/in ³	20/in ³

Table 2 Comparison of Channelizer Technologies

Technology Parameter	SAW Filter	SAW Steered	A/O Bragg Cell	BAW Steered	Dielectric Resonator	Lumped Element	MSW
Frequency (GHz)	0.25–1.25	0.25–1.0	0.5–4.0	0.5–10	5–15	0.2–2.0	1–20
Channel bandwidth (MHz)	5–100	5–30	2–20	5–100	10–50	20–100 ^a	5–100
Two tone dynamic range (dB)	50	40	36 ^b	40	> 60	> 60	50
Channel density (/in ³)	13	> 100 ^c	5–40	20–100 ^c	1–5 ^d	1–5	4–20
Availability	now	development	now	development	now	now	development

^aMinimum channel bandwidth is frequency.
^b> 50 dB achievable with interferometric detection.
^cDoes not include fan-out.
^dVolume is 1/frequency.

Fig. 12: (a): Insertion loss versus frequency for the device. Inset: 13-channel MSW filterbank. **Table 1:** The performance of the 13-channel filter together with projections on future performance. **Table 2:** Comparison of the filterbank/channelizer technologies. Adapted from [40].

of signal phase is essential for beam steering, signal synchronization, and interference mitigation. Their performance is characterized by phase shift range, insertion loss, and phase resolution, making them integral to the optimization of modern RF systems. RF phase shifters can be implemented using various technologies, including semiconductor (PIN diode-based or FET-based designs), MEMS, digital, etc. However, they all are subjects to the same limitations as filters described above - high insertion losses and power consumption beyond mid-5G bands, more complex, bulkier and expensive manufacturing process, etc. Phase shifting was one of the earliest application of ferrite materials, with early designs documented as far back as the 1956 [43]. Existing widely-used ferrite phase shifters (including those on YIG) do not use spin-waves for phase shifting, but are based on the magnetic field-induced change in the permeability of the ferrite material, which in turn alters the speed at which the electromagnetic wave propagates through the material (delay of the signal). The phase shift is a result of this change in propagation speed. While offering excellent power handling and wide frequency range, are often hindered by their size and slow operation magnetic field biasing.

Magnetostatic spin wave-based delay lines can often act like variable phase shifters (more on delay lines further in this *Section*). In the device demonstrated by Krug [185], the integrated antenna array consisting of five planar resonators were connected via microstrip to five equally spaced taps along an MSSW delay line. The transducers and array elements were fabricated on a 2-inch square alumina substrate. A permanent magnet provided the magnetic bias field, and beam steering was achieved by adjusting the bias field with an auxiliary coil. At 3 GHz, a scan angle of 35° was achieved with a 14 Oe

variation in the magnetic field.

An overview of MSW devices has also done by Kalinikos and Ustinov in book chapter [184]. Operational characteristics of the proposed nonlinear phase shifter based on surface SW are shown on Fig. 13. The device prototype was fabricated with two 50 mm wide and 2 mm long short circuited microstrip antennas evaporated onto a grounded alumina substrate of 500 mm thickness. The distance, d , between the antennas was 4.6 mm. The antennas were fed by microstrip transmission lines of 50 Ohm characteristic impedance. A 13.6 mm thick, 2 mm wide, and 40 mm long YIG single-crystal film strip was utilized in the nonlinear phase shifter. The film was grown by liquid phase epitaxy on 500 mm thick GGG substrate. The YIG film demonstrated a narrow ferromagnetic resonance linewidth of 0.05 mT at a frequency of 5 GHz and a saturation magnetization of 1947 G. The YIG/GGG was positioned with the YIG side down over the microstrip antennas. Fig. 13 displays a typical return loss versus frequency characteristic and an amplitude-frequency characteristic of the nonlinear phase shifter measured for the bias magnetic field of 143.1 mT for the different input power levels P_{in} from -6 to +23 dBm. For the small input power of 6 dBm, the SW propagated in a linear regime within the entire operating frequency range. During the increase in the input power, the return loss was varied by negligibly small values, whereas the insertion loss was considerably increased. In particular, the minimum insertion loss of -7 dB observed around the frequency of 6.34 GHz for powers up to +10 dBm was increased up to -15 dB with the increase in the input power up to 23 dBm.

Further experimental studies in this field were done by Hansen et al., [186] that proposed spin-wave phase shifter,

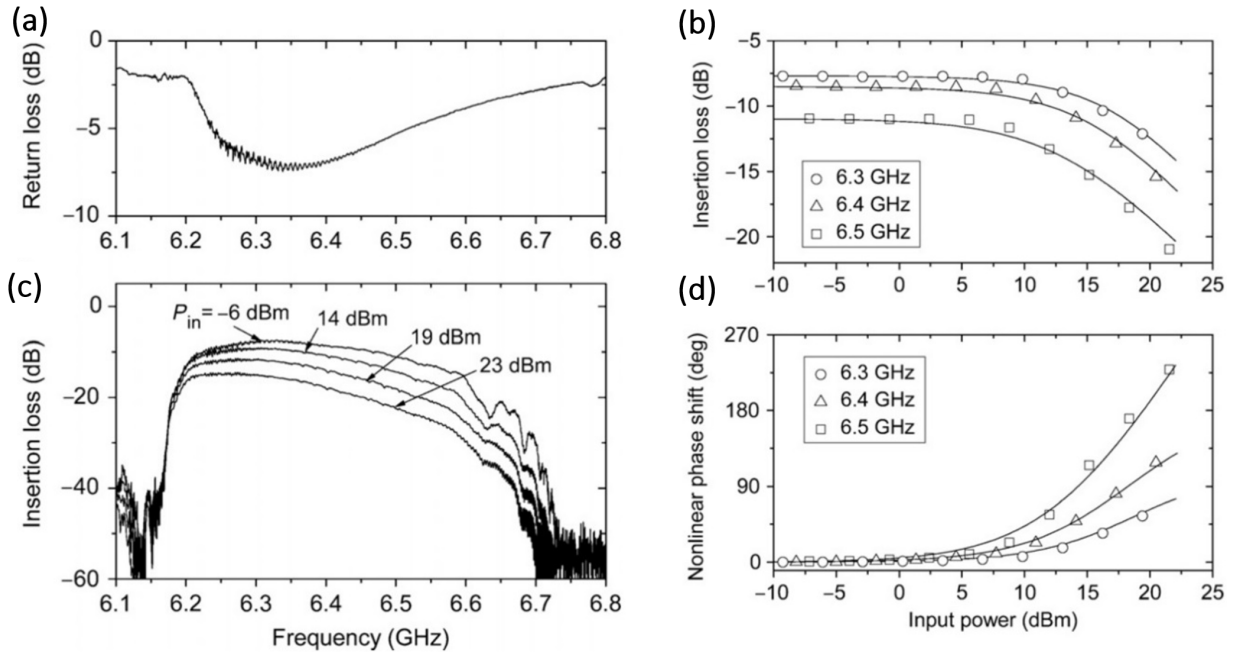


Fig. 13: Frequency characteristics of return (a) and insertion loss (c) of the nonlinear phase shifter measured for the different input powers P_{in} as indicated. Insertion loss (b) and differential nonlinear phase shift (d) measured and calculated for the different frequencies of 6.3 GHz, 6.4 GHz, and 6.5 GHz as a function of the input power. The symbols and the solid curves show experimental and theoretical data, respectively. Reprinted from [184].

capable of both linear and nonlinear control over phase accumulation. They demonstrated a device based on 6.1 μm -thick YIG stripe waveguide with lateral dimensions $1.5 \times 15 \text{ mm}^2$, where excitation and detection were done by 50 μm -wide antennas, placed 4.8 mm away from each other. Uniform biasing field of about 800 Oe was applied in the plane of YIG stripe, while local field modifications were done through a pulsed electric current flowing through a wire conductor centered between the antennae. Linear control is achieved by creating a local inhomogeneity in the external magnetic field, while nonlinear control relies upon the shift in the SW dispersion spectrum with increasing spin-wave amplitude. The study demonstrates that these two mechanisms can operate simultaneously within a single device, offering minimum cross-talk. This dual-functionality enables the realization of logic operations, enhancing the versatility and performance of SW-based RF and computing systems.

Latest advancements include the nanoscale spin wave valve and phase shifter, simulated by Au et al., [187]. The device is operating by integrating a nanomagnet atop a magnonic Permalloy waveguide, where the static magnetization direction of the nanomagnet controls its function. When a spin wave travels through the waveguide, it can resonantly excite the nanomagnet. Then, depending upon the static magnetization of the nanomagnet, it can either absorb spin-wave energy or alter its phase. This mechanism enables the device to serve as a controllable element in spin wave-based architectures, offering benefits like energy efficiency, non-volatility, and miniaturization.

The field of spin-wave phase-shifters is not so well explored as spin-wave filters, yet with advancements in miniaturization, it can be a competitive R&D topic.

D. Delay lines

RF delay lines introduce a controlled time delay (ranging from nanoseconds to microseconds) to electrical signals. Depending on the choice of propagation medium, delay lines can be realized using coaxial electric lines, SAW, BAW, integrated circuit components, etc. This delay capability is crucial for applications requiring precise timing, such as phased-array antennas, radars, and multi-band, multi-antenna 5G communication systems. The latter typically rely on SAW-based delay lines, which provide time delays in the range of 10 to 100 ns and a useful frequency range up to approximately 3 GHz. Above this frequency, insertion losses increase dramatically, leading to the conventional use of BAW-based delay lines. However, this solution also comes with a trade-off of shorter delay times (from a few nanoseconds to tens of nanoseconds), as bulk acoustic waves travel faster than surface acoustic waves. Additionally, BAW-based delay lines face technology-inherent challenges such as poor scalability, limited tunability, and increased losses at frequencies above 20-25 GHz. Switching to spin-wave technology offers an immediate solution by enabling longer delay times and the construction of more compact devices, as the group velocity of spin waves is much slower (and wavelengths shorter) compared to electromagnetic waves. Furthermore, the time delay in spin-wave-based delay

lines can be precisely adjusted by selecting the appropriate magnetic material, optimizing the spacing of the transducers, and controlling the applied magnetic field. This flexibility allows them to operate across a wide range of frequencies, which can be tailored to specific application needs [40], [42].

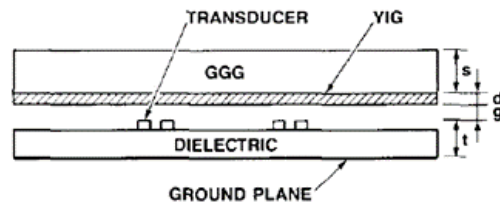


Fig. 14: Schematic of a SW delay line. Adapted after [42].

At any given bias magnetic field, the dispersion characteristics of a spin-wave (SW) mode are defined by the YIG film dimensions, including its thickness and width. For delay lines, these characteristics also depend on the spacing between the YIG film and both the ground planes and transducers. Spin-wave delay lines (e.g., Fig. 14) typically exhibit propagation losses of 23 dB/ μs at 9 GHz and 46 dB/ μs at 20 GHz [42]. Thus, for a delay line with a 200 ns delay, the insertion losses would be approximately 4.6 dB at 9 GHz and 9.2 dB at 20 GHz, assuming propagation losses are the primary factor. These values compare favorably to other delay line types, such as coaxial cables, where a 200 ns delay at 9 GHz would require a cable approximately 150 feet in length and yield at least 30 dB of insertion loss [42].

Magnetostatic wave delay lines for phased-array antennas [40] would be useful because of the wide instantaneous bandwidth obtained when real-time delay is used for beam steering [40], [188]. A lot of attention was dedicated to SW delay units based on two dispersive delay lines, an "up-chirp" (using FVMSW or MSSW) and a "downchirp" (using BVMSW) in cascade. Both delay lines have an accurately linear delay-versus-frequency characteristic, but with opposite slopes. The total delay is varied by changing the magnetic bias field applied to single, or both, delay lines. The maximum delay variation of 40 ns was shown with a 300 MHz bandwidth centered at 3 GHz. The rms phase error ranged from 8 to 13 degrees, and the insertion loss was 35 dB.

Variable magnetostatic wave delay lines were reviewed in 1985 by Bajpai et al., [189]. Experiments were carried on 5 mm-wide and 20 μm -thick YIG film separated by 635 μm -thick alumina wafer from the ground plane. 50 μm -wide golden transducers, deposited on the alumina, were separated by 1 cm. Importantly, applied field was rotated in two configurations - FVMSW - to MSSW and FVMSW to BVMSW. The time delay of this device was adjustable over a $\pm 20\%$ delay range and had a bandwidth of 150 MHz in 8-12 GHz frequency range with a transmission (insertion) losses around 20 dB.

E. Frequency selective limiters and signal-to-noise enhancers

Power limiters are crucial devices for protecting RF electronics from large input signals. Their purpose is to maintain

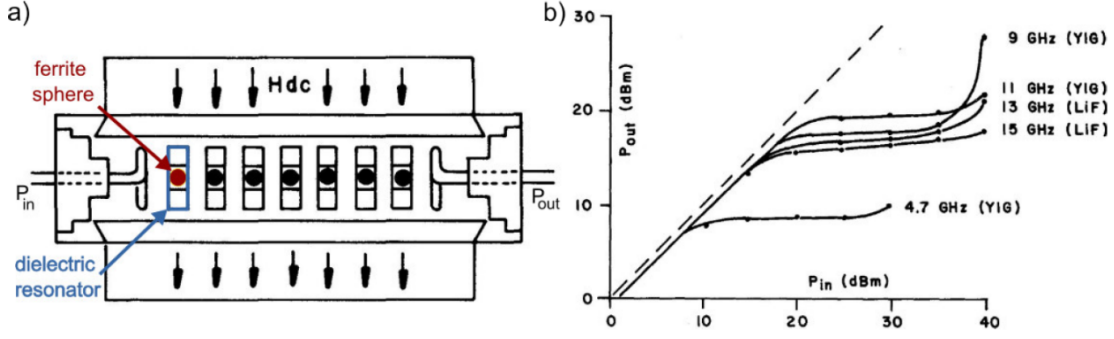


Fig. 15: (a) The experimental configuration of a power limiter consisting of a ferrite sphere resonator. (b) Measured limiting effect at frequencies of 13 GHz and 15 GHz for lithium ferrite spheres, and 4.7 GHz, 9 GHz and 11 GHz for YIG spheres. Reprinted from [171].

the output power at the constant power limiting level for the input powers above the power threshold. Conventionally used power limiters are based on semiconductors (diodes), as they are planar and CMOS compatible. However, when approaching the high GHz frequency, the semiconductor-based power limiters suffer from high electrical noise and switching delays. Moreover, when two signals at different frequencies and of different magnitudes are received, the semiconductor-based limiter attenuates these signals equally once a certain power threshold is reached.

In contrast, ferrite-based Frequency Selective Limiters (FSLs), which operate through spin-wave absorption or transmission, offer frequency-selective attenuation. Specifically, high-power signals at certain frequencies (above a set threshold) are suppressed, while low-power signals at different frequencies remain unaffected, thereby improving the signal-to-noise ratio. However, research on these devices has mainly focused on macroscale implementations (in the millimeter range) and frequencies below 15 GHz, primarily due to current technological demands. Nonetheless, FSLs are gaining increasing attention from the industry - relevant applications for these devices include Global Positioning Systems (GPS) [190], Mobile User Objective Systems (MUOS) [190], and communication networks for autonomous vehicles [191].

In 1974, Elliott, Nieh and Craig [171] built power limiter as a ferrite sphere resonator (Fig. 15(a)). The ferrite spheres were located in the dielectric cylinder resonators, which concentrated the dynamic magnetic field component in the middle of the cylinder. This magnetic field redistribution resulted in a lower power threshold. As a magnetic material for the ferrite spheres, lithium ferrite or YIG was used due to their narrow SW linewidth. The ferrite spheres were located in the external magnetic field created by a permanent magnet. In [192] the external field was about 210 mT and the resonator consisted of 28 YIG spheres. The insertion power loss was about 1 dB. The power-limiting effects are shown in Fig. 15(b) for lithium ferrite (frequencies of 13 GHz and 15 GHz) and for YIG spheres (frequencies of 4.7 GHz, 9 GHz and 11 GHz). Later, in 1980s, selective limiter (FSL or power limiter) and signal-to-noise enhancer (SNE) were realized from the epitaxial YIG films [40], [193] upon the principle of SW saturation at high-microwave power levels. Both devices achieved broadband operation and low-threshold

power levels. The limiter demonstrated a low loss for below-threshold signals and an increased loss for larger above-threshold signals, while the signal-to-noise enhancer – exactly the opposite characteristics. SW-based FSL can be used to extend the dynamic range of broadband microwave receivers, while signal-to-noise enhancer has a potential for frequency memory loop or keyed oscillator applications.

An operating principle of the mentioned MSSW-based FSL and SNE was thoroughly described by Zavislyak, et al. [34] (Fig. 16). Small signal inputs to the SNE result in the transduction of MSSW and, hence, attenuation of the signal in the microstrip line. The attenuation per unit length remains constant with increasing power until the threshold power level is reached (Fig. 16(b)). For the FSL, this threshold occurs due to the generation of half-frequency spin waves [34]. Thus, above threshold the MSSW power carried from the microstrip is approximately constant, and, hence, the attenuation in the microstrip line decreases with increasing input power. The MSSWs act as saturable absorbers of power from the microstrip line.

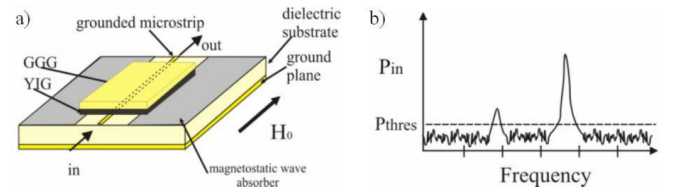


Fig. 16: (a) Signal-to-noise (SNE) enhancer and input power spectra with the (b) threshold level indicated. Adopted after [34], [193]

In a more recent work, Adam [173] demonstrated FSL operating in the 400 MHz to 800 MHz frequency range with a frequency selectivity and threshold power levels 100x lower than achieved with stripline devices (Fig. 17). The power limiter was based on a transmission of MSSWs under in-plane bias magnetic field of 1 mT. The author investigated three samples of different concentrations: undoped YIG, and YIG doped with scandium and gallium (ScGaYIG). Device shown the threshold power levels of around 20 dBm, narrow selectivity bandwidth 2 MHz and low intermod levels.

While an FSL usually relies upon MSSW, limiters utilizing hybrid MSSW/BVMSW for lower frequency operation have also been developed [34], [194]. In 2022, Yang et al.,

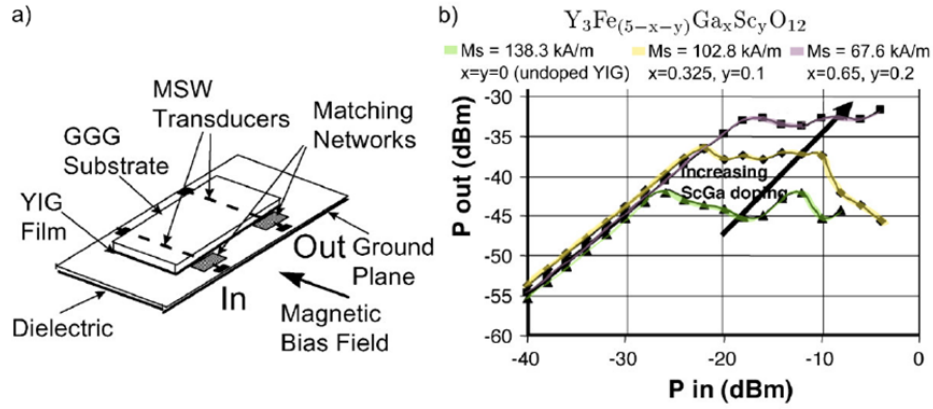


Fig. 17: (a) The frequency selective limiter configuration consisting of a YIG film placed on two conductors. (b) Measured limiting effect at unknown frequencies for undoped and doped YIG samples of different saturation magnetization of (green curve) 138.3 kA/m, (yellow curve) 102.8 kA/m and (violet curve) 67.6 kA/m. Adopted after [173].

[172] performed high-power MW pulse measurements in the absorptive-type microstrip YIG power limiter (Fig. 18). The sample was 300 μm thick, 12 mm wide and 50 mm long. The golden conductor for SW excitation was 17 μm thick, 190 μm wide, and 50 mm long. In the experiments, the external in-plane field of 82 mT was applied perpendicularly with respect to the longer side of the YIG stripe. When the high-power MW pulse of initial frequency was sent to the gold conductor, the SWs of half of the initial frequency were excited (causing the power limiting effect).

Just recently, in 2024, the first nanoscale power limiter based on spin-wave transmission affected by multi-magnon scattering in 97 nm thin YIG film was demonstrated. The antennas for the SW excitation and detection were 250 nm wide and 10 μm and 100 μm long. The devices were tested in the broad frequency range up to 25 GHz for both fundamental in-plane spin-wave modes - surface spin wave (here - Damon-Eshbach, DE) and Backward volume - see Fig. 19 and key parameters were obtained (insertion losses, power threshold, power limiting level, bandwidth). The lowest power threshold achieved were $-25.5 \pm 3 \text{ dBm}$ at 4 GHz and 9 GHz for

DE mode, and $0 \pm 3.5 \text{ dBm}$ at 25 GHz for BV mode using 10 μm long transducers. The lowest insertion losses in these proof-of-concept devices were 23 dB. A numerical model was developed to quantitatively describe the measured power characteristics, providing a pathway for reducing insertion losses. The paper also expertly summarizes advantages and disadvantages of the spin-wave power limiters, theorizing a three-in-one device that functions as FSL, delay line and filter simultaneously.

Alternatively approach was demonstrated by Wang et al., [196], who investigated power-limiting effects in YIG waveguide under the out-of-plane bias external field of 330 mT. The waveguide was 200 nm wide and 44 nm thin. Two micrometer-wide metallic antennas (10 nm Ti/150 nm Au) were placed over the waveguides for SW excitation. For a sufficient input power, the nonlinear FMR frequency was excited underneath the antenna. This resulted in conversion to self-normalized short-wavelength SWs in the vicinity of the antenna (Fig. 20). Therefore, the power-limiting effect, in this case, is based on a self-locking nonlinear shift. The results obtained in this paper are of great interest as they indicate that the filters/power

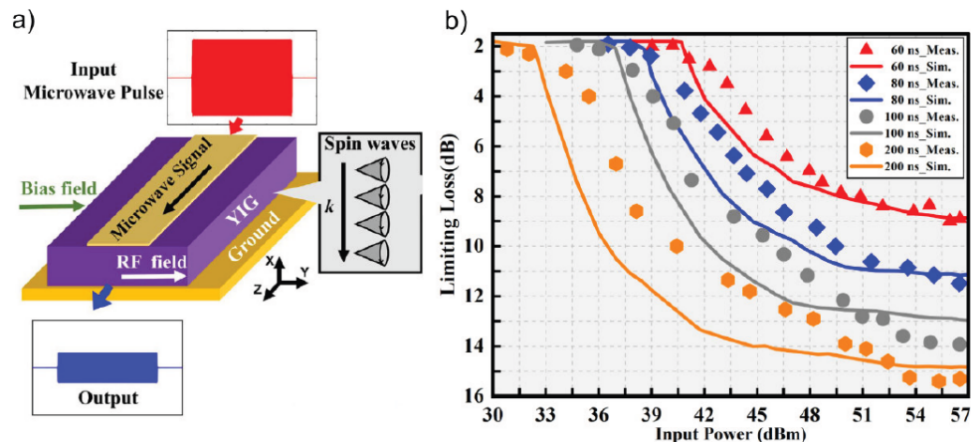


Fig. 18: (a) The experimental configuration consisting of a golden conductor at the top of the YIG stripe. (b) Measured (points) and simulated (curves) data for high-power MW pulses of different duration of 60 ns (red), 80 ns (blue), 100 ns (gray) and 200 ns (orange). Reprinted from [172].

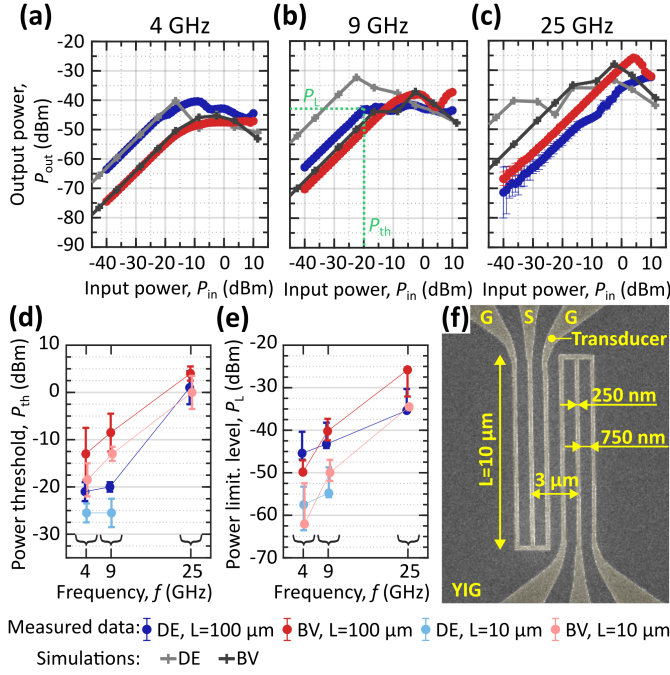


Fig. 19: (a)-(c) Extracted power characteristic from spin-wave power transmission in 97 nm thin YIG film measured using CPW antennas of the length $L=100 \mu\text{m}$. The power characteristics were measured and simulated for Damon-Eshbach (DE) mode in blue and light grey and for Backward volume (BV) mode in red and dark grey at a) 4 GHz, DE: 71 mT, BV: 87 mT, b) 9 GHz, DE: 244 mT, BV: 255 mT and c) 25 GHz, DE: 807 mT, BV: 823 mT. b) The power threshold and power limiting level for the DE power curve are indicated in green. Extracted d) power threshold e) power limiting level from power characteristics measured using CPW antennas of the length $L=100 \mu\text{m}$ (dark colors) and $L=10 \mu\text{m}$ (light colors) for both DE and BV modes. f) SEM image of fabricated CPW antennas of the length of $L=10 \mu\text{m}$. Adapted from [195].

limiters can be scaled down to nanometer size. This would allow for the use of ferrite-based RF devices in integrated circuits, where the optical BLS probe has to be replaced with another MW antenna.

A similar nonlinear effect of forward spin waves shift in nanoscale waveguides was explored in subsequent work by Wang et al., [197], where an all-magnonic repeater was developed. The device was based on a $1 \mu\text{m}$ -wide YIG waveguide supplied with a CPW source antenna and a pump strip antenna (repeater). The pump antenna enables two stable magnon states with high and low spin-wave amplitudes, and allows to switch between them. In a cascade logic system, for example, such a repeater would not only improve the damped input signal, but would also regenerate new spin waves with amplified amplitude (with the gain up to 6 times) and normalized phase to connect the next level logic gate. Such a design [197] allows for a simplified and robust magnonic circuits for a variety of applications. Although the last two articles are still more related to the fundamental academic research, the discovered physical phenomena allow the realization of devices and functionalities not available for any previously reported SW RF applications.

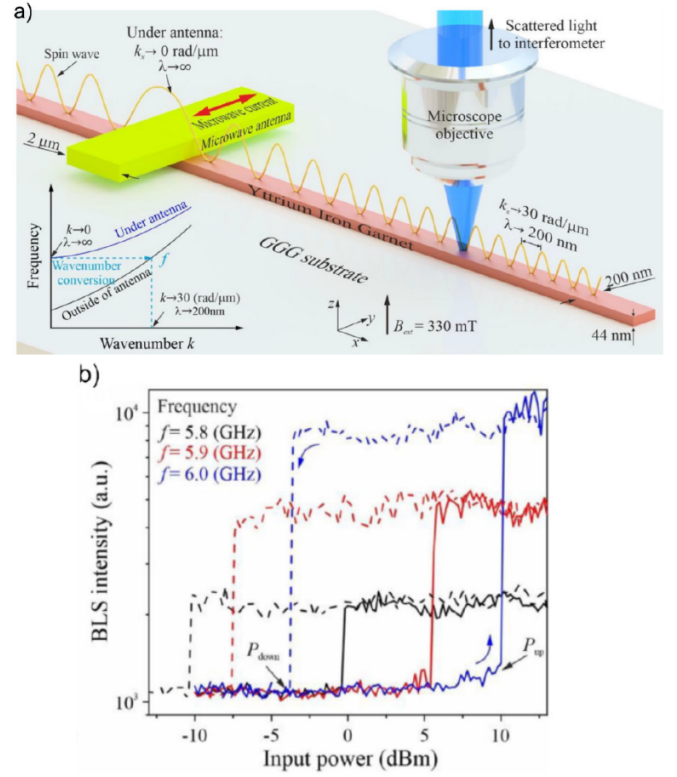


Fig. 20: (a) The experimental configuration consisting of a $2 \mu\text{m}$ wide microwave antenna placed over 200 nm wide YIG waveguide located in the out-of-plane external field of 330 mT. The nonlinear shift in the SW dispersion relation is shown at the bottom left. (b) Optically measured SW intensity at different frequencies of 5.8 GHz, 5.9 GHz and 6.0 GHz as a function of the input power up-sweep (solid curve) and downsweep (dashed curve). Adapted from [196].

F. Resonators

A resonator is a device or structure that naturally oscillates at specific frequencies, known as its resonant frequencies. When excited by an external signal or energy source at or near its resonant frequency, the resonator can store and sustain oscillations, often amplifying the signal within a narrow frequency band. Resonators are used in various applications, particularly in RF, microwave, optical, and acoustic systems, where precise frequency selection, filtering, or signal enhancement is needed. Magnetostatic spin waves are naturally excellent candidates for the resonators due to a high group velocity and the quality factor Q of MSW being theoretically frequency independent. Only 3 years ago, Dai et al., have designed, fabricated, and characterized magnetostatic wave (MSW) resonators on a chip [88] (Fig. 21). The resonators were fabricated by patterning single-crystal YIG film and excited by loop-inductor transducers. A thick aluminum coplanar waveguide inductor loop was fabricated around each resonator to individually address and excite SWs.

At 4.77 GHz, the 0.68 mm^2 resonator achieved a quality factor $Q > 5000$ with a bias field of 98.7 mT. The proposed device could be tuned with in-plane bias magnetic field by more than one octave from 3.63 to 7.63 GHz. The measured quality factor of the resonator is consistently over 3000 above

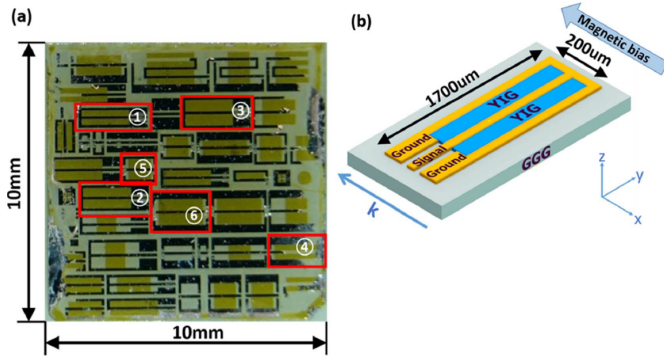


Fig. 21: (a) Top view of the chip with multiple MSW YIG resonators that are designed to operate from 4.54 to 4.58 GHz with the same 90 mT bias [Devices 1-6]. (b) Schematic of MSW resonator as marked in red. Reprinted from [88].

4 GHz [88]. The innovative design of a passive nanoscale spin-wave ring resonator was recently proposed by Wang et al., [198], yet its functionality was rather aimed as wake-up receiver in power critical IoT applications.

G. Directional couplers

A directional coupler is a passive RF component that splits an input signal into two output paths, typically with one path carrying the majority of the signal power (the through line) and the other carrying a small, sampled portion (the coupled line). Directional couplers are designed to sample signals with minimal impact on the original signal flow, enabling monitoring or measurement without interrupting the main signal path.

Directional couplers are usually designed using multistrip couplers and multiple YIG-film structures. Input and output microstrip transducers are located at both sides of the coupler, similar to SAW. Using two YIG films separated by a dielectric layer, MSSW propagating in one film will couple to the other film in such a way that the coupling is periodic with a distance along the propagation direction. Full power transfer has been achieved at 2.9 GHz using two 20 μm thick YIG films separated by a 250 μm thick dielectric layer [42]. The bias field can also be used to vary the amount of power transfer.

Due to the advancement in material fabrication and nanoscaling, Wang et al., designed, fabricated and tested a milestone spin-wave directional coupler [10], [199] based on the single-mode 350 nm-wide, 85 nm thick YIG waveguides. The information was carried by a SW amplitude, which was guided to one of the two coupler's (Fig. 22(a)) outputs according to the signal power (Fig. 22(b)), frequency (Fig. 22(c)), and the bias magnetic field. Thereby, this directional coupler can be considered as a universal all-magnon unit, allowing for the creation of fully functioning low-energy magnonic circuits. Physical origins of the selective transmission between the two conduits at distinct frequencies (Fig. 22(c)) is the frequency-dependent coupling length, which defines the distance where spin-wave energy is completely transferred from one waveguide to the other one. Furthermore, (Fig. 22(c)) demonstrates

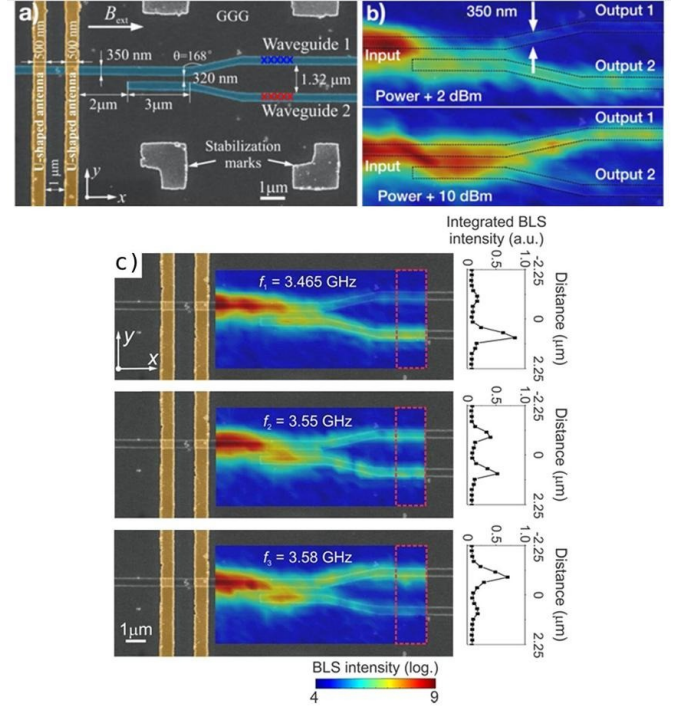


Fig. 22: Scanning electron micrograph of a directional coupler (shaded in blue). Bias magnetic field is applied along the YIG waveguide in the x-direction to saturate the directional coupler in a backward volume geometry. (b) Nonlinear transfer characteristics of a nanoscale directional coupler. The color maps represent the two-dimensional spin-wave intensity distributions measured by Brillouin Light Scattering (BLS) microscopy for input powers of 2 dBm (top) and 10 dBm (bottom). (c) Two-dimensional BLS maps (the laser spot was scanned over an area of $9.4 \times 4.5 \mu\text{m}^2$ by 30×20 points) of the BLS intensity for c) top: $f_1 = 3.465$ GHz, c) middle: $f_1 = 3.55$ GHz, and c) bottom: $f_1 = 3.58$ GHz. The right panels show the spin-wave intensity integrated over the red dashed rectangular regions at the end of the directional coupler. Reprinted from [10], [199]

the potential use of such a directional coupler as a frequency division demultiplexer, e.g., different frequencies applied to the same input of the directional coupler are transferred to different outputs of the device. In addition, a magnonic half-adder concept, consisting of two directional couplers, was simulated using a micromagnetic solver and benchmarked against a 7 nm CMOS half-adder [10]. The results indicate that the proposed concept, miniaturized down to 30 nm in width, 10 nm in thickness of YIG waveguides, can have a footprint comparable to CMOS half-adder, with around 10x smaller energy consumption [10].

H. Selected spin-wave RF patents

Innovative spin-wave RF devices are well documented through the US and European patent base, highlighting advancements in the use of spin waves for efficient signal processing and communication applications. According to the Patent Public Search PPUBS Basic, over the last two decades the number of patents that included key words "spin-wave" and "RF" has progressively increased in around 9 times comparing to the period 1960-2000.

In particular, patents related to spin-wave filters often rely on a magnetostatic spin waves (MSW) in magnetic ferrites [e.g., Geho et al., 5,985,472, 11/1999 - 08/876,555; Geiler 11,349,185 B1, 5/2022 - 16/871,553]. For example, Murphy et al. [5,955,987 A, 9/1999 - 342/357.06] patented an adaptive RF filter based on Yttrium Iron Garnet (YIG) thin ferrite film positioned transversely between input and output stripline transducers. When subjected to an external magnetic field, the device operates as a signal delay line with variable impedance, where a spin wave is used to absorb excess energy above a set threshold from signals applied to the input transducer. This threshold is adjustable and depends on the thickness of the YIG film. Correspondingly, Adam et al., proposed MSW-based frequency-selective limiter design [6,998,929 B1, 2/2006 - 0/424,738] using a pair of parallel microstrip transducers on a substrate. The transducers have a length at least equal to the width of the overlaying YIG film, which ranges in thickness 0.1 μm to 5.0 μm and has a width of up to 20 mm. The device is biased by a permanent magnetic field applied in the plane of the YIG film, parallel to the transducers, enabling magnetostatic waves to propagate between them. This configuration provides a low-threshold power frequency selective limiter with a threshold power ranging between -75 dBm to -35 dBm. It is particularly useful in GPS systems, where such FSL ensures jammer-free and interference-free operation for RF receivers, as well as in airborne, surface, or other vehicle platforms for accurate position computation.

Correspondingly, Chumak et al., proposed an innovative filter design and process for filtering radiofrequency signals [European Patent Application No. EP23200651.0. The patent will be opened on 28.03.2025]. Device uses nanowaveguides instead of planar YIG films, leading to the dilution of the magnon mode spectrum and suppression of the multi-magnon scattering processes, providing an additional independent parameter to tune the threshold power. The gaps in between the nanowaveguides are proposed to be used for the deposition of permanent micromagnets [200], [201], [202], that would magnetize YIG, enabling the tuning of operational frequencies for specific applications.

Alternatively, spin-wave FSL can be realized from magnonic crystals - spatially periodic magnetic structures - adapted for selectively filtering a spin wave spectral component (e.g., a bandwidth, a filter peak frequency, a phase shift, a notch frequency, and/or another controllable spectral parameter) of a spin wave propagating through the waveguide,

as proposed by Ciubotaru et al., [10,033,078 B2, 7/2018 - 15/604,314].

Another notable patenting direction involves spin-wave transducers for high-performance spin-wave devices at microwave and millimeter-wave frequencies [e.g., Aquino et al., US 2023/0299451 A1, 09/2023, 18/185,756].

These developments highlight the growing potential of spin-wave technology in next-generation RF systems, offering improved efficiency, miniaturization, and performance compared to traditional electronic counterparts.

IV. ADVANTAGES AND CHALLENGES OF SPIN-WAVES FOR RF APPLICATIONS

A. Advantages

The field of magnonics draws special interests from the scientific community and industry's R&D departments due to the unique combination of the intrinsic properties of spin waves:

- **Scalability of the devices from centimeters down to nanometers.** Since the minimum sizes of wave-based elements are defined by the operating wavelength λ , the lateral sizes of devices can range from cm, as in classical MSW-based devices [9], [10], [173], to sub-100 nm, as recently reported [10], [81]. The smallest possible spin-wave wavelength is limited only by the lattice constant of a magnetic material, and, consequently, is in the angstrom range. As highlighted in [195], SW technology, naturally confined to the magnetic material, allows for an easy planar device design, facilitating on-chip integration. For example, a chip containing multi-channel frequency-selective limiters can have a footprint below $1 \times 1 \text{ mm}^2$ with a working areas of individual devices less than $10 \times 100 \mu\text{m}^2$ [195] **Therefore, one of the major advantages of SW-based technologies over MW-based devices is the ability to independently miniaturize sizes by at least three orders of magnitude or more in the desired frequency range.** For better understanding, please refer to the Table I, where the electromagnetic wave and spin wave (dipolar dominated MSW and exchange dominated SW) wavelengths λ have been calculated for 5 μm thick YIG film in BV geometry, with the corresponding bias magnetic field value given in the last column. Reciprocally, it can also be stated that **SW devices are universal units, capable of adapting to a wide**

TABLE I: Comparison of the frequency-dependent electromagnetic wave (EMW) and spin wave wavelengths λ calculated for 5 μm thick YIG film in backward volume (BV) geometry.

Frequency	Wavelength λ			
	EMW	Magnetostatic (dipolar) SW	Exchange SW	Magnetic field
1 GHz	30 cm	$\sim 10 \mu\text{m}$	$\sim 200 \text{ nm}$	10 mT
10 GHz	3 cm		$\sim 70 \text{ nm}$	10 mT
		$\sim 10 \mu\text{m}$	$\sim 200 \text{ nm}$	300 mT
50 GHz	0.3 cm		$\sim 30 \text{ nm}$	10 mT
			$\sim 40 \text{ nm}$	300 mT
		$\sim 10 \mu\text{m}$	$\sim 200 \text{ nm}$	1.75 T

frequency spectrum without requiring physical scaling - check Table II and next bulletpoints. In contrast to SAW and BAW devices depending on miniaturization to achieve higher frequencies, SW devices have an edge in compactness, flexibility and scalability of RF applications, especially in mobile communication sector.

- **Ability to tune spin wave wavelength, frequency and velocity independently.** Spin wave characteristics can be varied by a wide range of parameters including the choice of the magnetic material, the shape of the sample, SW mode selection, as well as the orientation of the applied biasing magnetic field [6], [7] together with transducers design. Many parameters of spin-wave RF devices are defined by these interconnected parameters, e.g., the center band frequency of an RF filter is given by its frequency range defined by the spin-wave dispersion, the size of spin-wave transducers and devices in general is dictated by the spin-wave wavelength and required bandwidth, the delay time is given by the spin-wave velocity and can be adjusted via the spacing between transducers and/or the thickness of the magnetic film. As highlighted by Davidkova et al., [195], the threshold power is also tunable through the choice of SW mode, transducer configuration, and materials, while dynamic econd tunantuning can be achieved with variable magnetic or electric fields in specific hybrid structures. This enables rapid adjustments of frequency-selective limiter (FSL) or filter passband frequency and bandwidth [195]. Hence, the ability to operate with multiple independently tunable parameters, offers a high flexibility for RF applications.

- **Low noise and tunable power threshold.** Following the previous point, we want to underscore specifically the lower noise in spin-wave devices at high frequencies compared to semiconductor ones. Good signal-to-noise ratio in combination with low power thresholds makes SW technology attractive for GPS applications [195]. Using nano-waveguides can further tune the power threshold by suppressing multi-magnon scattering, as proposed in a recent patent [European Patent Application No. EP23200651.0. The patent will be opened on 28.03.2025].

An example of SW flexibility is shown in Table II: the same SW wavelength λ of 2 μm could be excited at different frequencies by applying different bias magnetic fields. The calculations were performed for a 5 μm thick YIG film in BV geometry.

TABLE II: Dependency of SW wavelength on frequency (magnetic field).

Frequency	Wavelength λ	
1 GHz	2 μm	30 mT
10 GHz	2 μm	350 mT
50 GHz	2 μm	1.78 T

- **Compatibility with existing industrial technology and standards.** Following the train of thoughts from the previous two bulletpoints, one can conclude that an **inexpensive and industrially-attractive conventional photolithography can be used for spin wave RF devices of any selected 4G and 5G operational RF frequency range**. Spin wave RF technology, based on propagating spin waves, has always been based

on **commercially attractive and CMOS-complementary planar technology** (using, e.g., chiplet concept [203]). The change SAW \rightarrow SW is technologically much easier than SAW \rightarrow BAW.

- **No need in isolation.** Furthermore, SWs are naturally confined by the magnetic material and, unlike SAWs or BAWs, signals in SW devices cannot propagate into the substrate or leak to neighboring circuits. **This makes spin-wave technology more industrially attractive and compatible.** The Bragg reflectors used in SAW resonators in conventional filters can also simply be replaced by the flat edge of the magnetic waveguide, resulting in perfect reflection of the spin waves.

- **Wide frequency range from sub-GHz to THz.** Modern information and communication technology systems such as cellular networks, Bluetooth, Wi-Fi, etc. operate in the 4G/5G frequency bands. Boolean computation is also performed in the GHz frequency range, with a benchmark overclocked frequency in a cryobath peaking at 8.5 GHz [204]. Although, in the laboratories, the typically used frequency range for spin waves is 1 to 20 GHz, the magnon spectrum spans several orders of magnitude in frequency from hundreds of MHz to the very promising THz range. The frequency is limited only by the Brillouin zone boundaries of the chosen magnetic material and the strength of the applied magnetic field. For example, in YIG, the material of choice for many RF applications, the magnon Brillouin zone is limited at about 7 THz [74]. Thus, **the same magnonic RF application can fully meet the requirements of 4G, 5G and future 6G technologies.**

- **Low energy transport loss and heat dissipation.** Typical materials for SW-based applications are insulators (e.g., YIG). Since a magnon current does not involve the motion of electrons, it is free of Joule heat dissipation. Therefore, SWs can propagate over distances larger than cm [9], while an electron-spin current has a much shorter span of μm with a limited spin diffusion length [205]. The values of the loss per time (e.g., reported 23- and 46-dB/ μs propagation losses at 9 and 20 GHz, respectively [42]) are given by the Gilbert damping parameter α and the operating frequency. However, it is often important to translate this loss into the loss per distance, which is also defined by the spin-wave group velocity. The velocity is consequently tuned by the saturation magnetization of a magnetic material and the film thickness for MSW, and by the exchange constant of the material for exchange spin waves.

- **Pronounced (controllable) nonlinear phenomena.** In order to process digital information, nonlinear elements are needed so that one signal can be manipulated by another (like semiconductor transistors in electronics). Spin waves have a variety of pronounced nonlinear effects that can be used to control one magnon current by another, for suppression or amplification [6], [7], [9], [206]. Such magnon-magnon interactions have been used to realize magnon transistors, and they open the door to all-magnon integrated circuits [10], [55]. From the point of view of RF applications, the natural nonlinearity could play a positive role, since it allows the realization of power limiters and signal-to-noise enhancers.

TABLE III: Comparison of the phase shifter technologies. Reprinted after [35].

	Ferroelectric	MEMS	Semiconductor	Ferrite (waveguide)	Ferrite (microstrip)
Cost	Low	Low	High	Very high	Low
Reliability	Good	Good	Very good	Excellent	Excellent
Power handling	> 1 W	< 50 mW	> 1 W	~ 1 kW	> 10 W
Switching speed	~ ns (limited if high voltage)	10 - 100 μ s	< ns (low power)	10 - 100 μ s	< 10 μ s
Radiation tolerance	Excellent	Excellent	Poor (good if hardened)	Excellent	Excellent
DC power consumption	~ 1 μ W	Negligible	< 10 mW	~ 10 W (~ 1 W latching)	< 10 μ W
Microwave loss	~ 5 dB/360° K band	~ 2.3 dB/337.5° Ka band	2 dB/bit band Ka band = 8 dB	< 1 dB / 360° X band	< 2 dB / 360° C-Ku bands
Size	Very small	Small	Small	Large	Small

On the other hand, nonlinearities also play a negative role, since it limits the maximum operating power of RF devices. Nevertheless, nonlinear magnon physics is very versatile, allowing the control of nonlinear parasitic processes.

- **Fast reconfigurability of parameters.** The SW dispersions can be controlled by the magnetization orientation, applied electric current or electric field, allowing access to reconfigurable RF devices with a 1 ns transition timescale. In principle, the same spin-wave RF device can have different functionalities, and **the function, as well as the device parameters (e.g., the center frequency of a pass-band filter) can be reconfigured on the ns scale.**

- **Broad scope of RF functionalities and the possibility to integrate them.** Spin waves have been used [34], [35], [40], [41], [42], [43], [44], or have the potential to be used [9], [14], [105] for the realization of a very wide range of passive and active RF devices: **pass-band and stop-band RF filters, resonators, phase shifters, delay lines, (de-)multiplexers, directional couplers, isolators and Y-circulators, power limiters, signal-to-noise enhancers.** For more complex RF systems, these functions can be integrated or dynamically switched in a single universal device.

B. Areas of concern in RF applications

The key mentioned concerns in spin wave RF application are listed below:

- **Insertion loss.** As discussed earlier, there are two concepts of spin-wave RF applications: the one in which the signal remains in the form of an electromagnetic wave, while magnetic media are used to absorb or reemit the microwave signal. In this case, the insertion losses are usually in the range of 1 to 3 dB (see Figs. 7-8) and are mainly determined by the quality of the microstrip-based microwave engineering and by the reflection of the microwave signal from the region where the magnetic structures are placed. The proper microwave design of the microstrip lines and the dielectric spacing between the metals and the magnets gives enough freedom to optimize the transmission characteristics and to minimize the parasitic losses. The second approach is based on the

excitation of propagating spin waves, their transport over a certain distance and spin wave detection (a back-conversion from a spin wave to an electromagnetic wave). The insertion loss in this case is higher, typically in the range of 6 to 20 dB. Probably one of the smallest reported insertion loss is shown by Zavislyak, Bobkov, et al., [34], [45] – around 2.5 dB (Fig. 10), and Wu, et al., [178] – around 1.7...2.4 dB (Fig. 11). As it was analyzed in *Section II.A*, the efficiency of microstrip converters in the former case is over 80%. Other examples of the relatively small insertion loss – 6 dB – are given in Fig. 13 [184] while discussing losses vs operating microwave powers, and in [207], where a new method for the computation of the insertion loss of MSSW transducers is discussed.

- **High power capacity.** If to consider the maximization of operational powers of the spin wave RF devices, one has to split the two approaches of SW RF applications as discussed above. In the approach where the energy is kept within the electromagnetic wave, the operational microwave power can be from tens of watts and up to kilowatts – see Table III [35].

If to speak about the spin-wave RF devices based on the propagating waves, then the increase of the input high-frequency power might lead to the excitation of SW nonlinear mode, similar to the power limiter devices above. Although this ability makes devices such as the already mentioned power limiters, signal-to-noise enhancers, etc., possible, yet for most passive RF units nonlinearity is undesirable as it limits working dynamic range of a device and deteriorates its characteristics.

YIG is a magnetic material with pronounced nonlinear magnetic properties. These properties reveal themselves stronger for films with smaller magnetic losses, defined by FMR linewidth. For example, as shown in Fig. 15(b), deviation from a linear input-to-output power relationship can take place already at input powers of around – 20 dBm for specialized power limiters. Based on academic experiments [9], it is possible to ensure operation in the linear regime for input microwave power levels up to 10 dBm – see Fig. 23 [208].

- **Linearity.** Passive spin wave RF devices, like delay lines and phase shifters, which also require the linearity in their operational characteristics, are usually called nondispersive delay

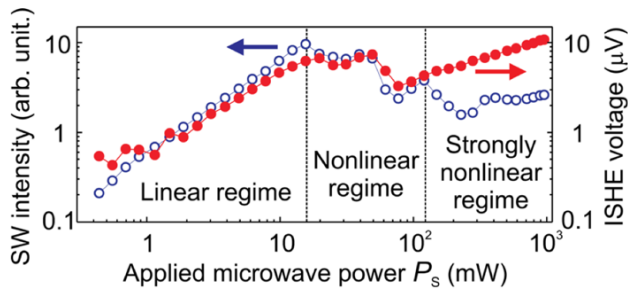


Fig. 23: Transmitted spin-wave intensity (open blue circles) and ISHE voltage (filled red circles) as functions of the applied microwave power P_s . Reprinted after [208].

lines [42]. Nondispersive, wide-band MSW delay lines could be a potential replacement for phase shifters and coaxial cables at MW frequencies. Examples of such applications are delay-line discriminators which require low-loss delay lines with 50-500 ns of delay. According to Ishak [42], by adjusting YIG film thickness and YIG/ground plane separation, it is possible to widen the band over which the ground delay is flat, and then use the bias field to center this band around the operating frequency [209], [210]. As stated in [42], by adjusting the bias magnetic field, the time delay for the composite device can also be controlled. Using a MSSW/BVMSW composite device, Sethares et al., [211] obtained ± 8.4 ns delay variations over a 200 MHz bandwidth at 3 GHz center frequency. It is important to keep the insertion losses of both delay lines as low as possible to produce a reasonably low loss for the composite device. Another approach to controllable nondispersive delays, according to [42], includes applying the bias field at an angle to the YIG film in a normal FVMSW delay line. At 9 GHz, Bajpai et al., [212] obtained 520 ns of delay variations at a nominal delay of 100 ns.

- **Trade-off in high frequency requiring high magnetic field.** This issue was emphasized by Davidkova et al., in a recent cutting-edge studies [195]. It was pointed out that to operate in a frequency region above 20 GHz, a magnetic biasing field above 700-800 mT is required. While this may not pose significant challenges in laboratory settings, it becomes impractical for industrial applications.

C. Strategies to overcome the concerns in RF magnonics

There is no existing recipe of a universal solution to all existing issues in applied RF magnonics - a step towards addressing one challenge might be a step backwards for the other, as discussed further. Yet, considering the progress in the recent developments (Chapter I C.) and the interest of both the scientific community and tech sector, fueled by the existing market demand, a compromise solution tailored to fit the pending requirements is on its way. The most immediate pathway for spin-wave (SW) technology to be integrated into commercial RF solutions lies in developing direct, one-to-one replacements for existing components. For example, an SW-based phase shifter module that meets the port and perfor-

mance specifications of traditional RF device can be adopted almost instantly with minimum additional adjustments.

Below, we will address separate potential solutions that address one specific area of concern:

Issue: Insertion loss.

Here we discuss only the concept in which the propagating spin waves are excited and detected by the two spatially separated SW transducers, since this approach suffers the most from the insertion loss (1.7... 2.5 dB are probably the best reported values). The ways to address this specific challenge currently are:

- **Increase the thickness of YIG films.** The excitation and detection efficiencies are primarily defined by the saturation magnetization of a magnetic material and by the volume of magnetic material interacting with the electromagnetic field of the antenna. Thus, the proper choice of the film thickness can increase the transducer efficiency. In addition, the group velocity of MSWs is practically linearly proportional to the thickness of the YIG film. Thus, increasing the thickness reduces the loss of spin wave energy that propagates between the antennas by decreasing the transmission time.

- **Selection of magnetic material with higher value of saturation magnetization.** Alternatively, another magnetic material with larger saturation magnetization compared to YIG (e.g., metals like Permalloy, CoFeB, etc.) might be used. In such a case, both the efficiency of the spin wave transducer and the group velocity of the MSWs should increase. However, the disadvantage of such an approach is related to the increased losses due to worse characteristics of the spin wave transport in comparison to YIG and YIG-based compounds, as YIG remains a champion material in terms of low spin wave losses.

- **Engineering more efficient transducer antennas.** As described above in the Sections I D. and II A. transducers, especially in micron-sized devices, should be optimized to reduce the ohmic losses and, consequently minimize the insertion losses. This can be accomplished either by reverting to a large external matching network, by significantly reducing the available bandwidth or by a proper numerical description of the complex circuit-level model including micromagnetics of the magnetic film. In particular, numerical proposed and experimental confirmed by Erdelyi et al., [131] corresponding IDT optimization model allowed to reduce the insertion loss below 5 dB over a 100 MHz frequency range in a structure composed of a 800 nm thick YIG film and two CPW antennas. At the micrometer scale, ohmic losses are largely dissipated as Joule heating, even with matched characteristic impedance of the antennas. High transduction efficiency is feasible only if these losses remain negligible compared to radiation resistance. For short wavelengths requiring narrow waveguides, high losses are unavoidable due to increased resistance, creating a trade-off between device scalability and insertion loss. However, for magnonic wavelengths above a few micrometers, low insertion losses can be achieved following the design dictated by the model [131]. Therefore, even from the standpoint of IDT,

magnonic RF devices offer significant promise in frequency ranges where traditional MW components face limitations.

- **More complex tools for numerical simulation.** To further boost the development of new and optimization of existing SW transducers, a conceptually novel approach to numerical simulations is required, in which the micromagnetic approaches would be combined with Maxwell solvers to simulate eddy currents. For further enhancement, the simulation tool might be fused with machine learning-based inverse design options for optimization and development of new transducer topologies. The development of such a numerical approach is currently on-going in the magnonics community.

- **Engineering the distance between the spin-wave transducers.** The simplest way to reduce the insertion loss contribution from the SW decay is to reduce the distance between the input and output transducers. However, an obvious drawback to this approach is direct electromagnetic leakage, which will occur between the transducers (i.e., the RF signal is not transmitted as a spin wave, but as a direct electromagnetic wave) when the distance becomes sufficiently short. For a filter, this leakage reduces the out-of-band attenuation. However, parasitic leakage can be suppressed by a proper antenna design. For example, the meander antennas discussed above have a very low microwave emission outside the antenna area and should reduce the leakage. As for the delay lines, the delay can be increased by decreasing the distance between the transducers. However, this can be compensated by engineering other parameters, e.g., the velocity of the MSW can be reduced by decreasing the thin film thickness.

- **Engineering of magnetic film waveguide.** The shape of the magnetic thin film can also be optimized. For example, in academic studies [9], where insertion losses are not critical, a simple YIG waveguide of about 2 mm width is used. The same approach was used in [184] – see Fig. 13. However, the size and shape of the sample is very different in the insertion loss-optimized device of Zavislyak – see Figs. 10, or as shown by Wu et al., – Fig. 11. Thus, the shape and configuration of the magnetic waveguide is another parameter that can be used to reduce the insertion loss.

Issue: High power capacity.

Again, we will only discuss the approach where the propagating spin waves are excited and detected by the two spatially separated spin-wave transducers. These devices can usually operate with limited applied microwave powers due to multi-magnon and parametric parasitic scattering processes [6]. The publicly disclosed potential ways to address the challenge are:

- **Engineering of magnetic film waveguides and use of multiple waveguides.** Under the simplest assumption that the critical point is not the absolute value of the energy transferred by the spin wave, but the density of the energy per unit volume, the solution would be very simple: to use SW waveguides of greater width and thickness to dilute the energy over the larger volume of magnetic media. Alternatively, an array of non-interacting MSW devices can be used to distribute the

applied energy among the identical devices.

- **Engineering of spin-wave transducers with small magnetic field strength.** An additional degree of freedom is the engineering of larger or specially shaped spin-wave antennas, which for the RF signal of the same applied microwave power will induce magnetic field around the antenna of smaller strength. A smaller magnetic field will consequently excite a smaller angle of precession in the spin wave, and thus the threshold of nonlinear magnon scattering will be reached at higher absolute values of the applied microwave signal.

- **The solution to suppress nonlinear multi-magnon scattering processes.** One way to minimize the nonlinear processes that appear at high MW powers (i.e., multi-magnon scattering process) is to decrease the thickness of magnetic thin film. For all the scattering processes, the energy and momentum conservation laws have to be fulfilled. The probability of fulfilling these laws, determined by the density of magnon states, specifies the probability of multi-magnon scattering. Therefore, when the dispersion spectra are diluted due to the mode quantization in width or thickness, there are fewer possibilities for fulfilling the energy and momentum conservation laws, resulting in a suppression of multi-magnon scattering. This was proven in the works of Jungfleisch et al., [132] on nm-thick YIG waveguides by inverse spin Hall effect studies. The effect of widening of the FMR linewidth with the increase in the operational microwave power, which is a signature of the parasitic nonlinear processes, was decreasing for films of smaller thickness. Therefore, the YIG thickness should be properly designed to suppress the parasitic scattering while maintaining high transducer efficiency.

- **Selection of magnetic material with higher value of Gilbert damping.** The majority of nonlinear scattering processes have a threshold where the energy induced into a spin wave mode is greater than the energy going to dissipation [6]. In practice, this means that the higher the attenuation of the magnetic material used, the higher the operating power of the RF devices. If we talk about the approach in which the data is conserved within the electromagnetic wave, the large damping should not have many drawbacks and commercially attractive materials, such as Py (permalloy) can be used. When talking about the RF devices based on the SW propagation over some distance, the increase in damping is not desirable. However, it can be partially compensated by increasing the velocity of the spin wave, e.g., by increasing the thickness of magnetic film. If we are talking about insulating low-damping YIG, then a potential solution to increasing the operational powers of RF devices would be to use cheap and commercially attractive polycrystalline YIG or doped YIG, which are known to have larger Gilbert damping parameters.

Issue: High linearity.

As discussed above, the realization of nondispersive, wide-band MSW delay lines with linear characteristics have been in the focus of classical studies on MSW RF application en-

gineering [42]. Many successful approaches have been found already, and similar ideas can be projected onto new materials or designs of RF devices.

- **Adjusting the YIG film thickness and the YIG/ground plane separation.** Using such an approach, it is possible to flatten the dispersion for MSW waves and to widen the band over which the ground delay is flat [209], [210].

- **Engineering nonuniform biasing magnetic field or saturation magnetization.** In principle, spin wave dispersion can be engineered by using a magnetic medium with non-uniform properties. It can simply be nonuniform across the width of the waveguide due to a biasing magnetic field or saturation magnetization, which can be achieved today using versatile techniques [213]. This approach would rely heavily on the micromagnetic simulations discussed in the next section. A simpler and already tested approach includes applying the bias field at an angle to the YIG film in a normal FVMSW delay line, as it was done by Bajpai et al. [212].

- **Using MSSW/BVMSW composite device.** Dispersive distortions in the operational characteristics of spin-wave RF devices take place due to the nonzero second derivative in the dispersion curve, resulting from the fact that spin waves at different frequencies have slightly different velocities. Nevertheless, the second derivatives have different signs in the BVMSW and MSSW configurations. Thus, one can achieve linear transmission characteristics by combining MSSW and BVMSW devices in line as it was done by in [211].

- **The use of exchange spin waves of high wavenumbers.** The classical spin-wave RF devices operate with MSW of relatively small wavenumbers (still orders of magnitude higher than the wavenumbers of electromagnetic waves). Nevertheless, modern techniques allow the operation with exchange spin waves of large wavenumbers [14], [105]. Exchange waves have a linear dispersion curve, but from a certain value (about 1/4 of the Brillouin zone) the dispersion curve starts to be almost linear [104]. Spin-wave operation in this range would allow the realization of non-dispersive and broadband RF devices. Nevertheless, a theoretical estimation has to be made, as it could be that the operating frequencies of such a device for YIG will be already in the hundred GHz range.

- **The use of active delay line devices and solitons.** There is a certain class of devices in which various types of amplification mechanisms, such as parametric pumping [10], are used [214], [215]. Another possibility how to obtain a nondispersive MSW delay line is to use magnetic solitons, as they overcome dispersion spreading [216], [112]. Magnetic solitons are highly stable and once generated by sufficiently strong microwave pulses, they can propagate over long distances at constant velocity maintaining their shape (they do not spread their energy). This stability is caused by the compensation of the nonlinear and dispersive effects.

Issue: High magnetic field

As stated earlier in the *Section I* and in [195], this issue can be solved by using alternative materials with strong crystallographic anisotropy, like Ga-substituted YIG with perpendicular magnetic anisotropy or M-type hexaferrites, depending on the frequency region required to achieve. If to consider high frequencies pushing 6G region, BaM is especially favorable candidate due to the high operating frequencies > 50 GHz and low losses in a high frequency range for moderate magnetic fields of < 1 T.

ACKNOWLEDGEMENTS

The project is funded by the FWF project PAT 3864023 "IMECS" and FWF ESPRIT Fellowship Grant ESP 526-N "TopMag".

AUTHOR CONTRIBUTIONS

KOL developed the review concept and authored the initial draft of the manuscript. KD provided crucial support through scientific discussions and insights into cutting-edge research. JM contributed a unique perspective from the tech industry, assessing the practical application potential. AVC conceptualized the review framework, proposed innovative concepts, and spearheaded the SW RF application research direction. All authors collaboratively contributed to refining and finalizing the manuscript.

COMPETING INTERESTS

The authors declare no competing interests.

Data availability: All cited data is an intellectual property of the original authors, and we claim no rights on them. The data that support the original section of the report dedicated to discussions are available from the corresponding author upon reasonable request.

REFERENCES

- [1] Delsing, P. et al. "The 2019 surface acoustic waves roadmap". *J. Phys. D: Appl. Phys.* **52**, 353001 (2019). URL <https://iopscience.iop.org/article/10.1088/1361-6463/ab1b04/meta>.
- [2] Ilderem, V. "The technology underpinning 5G". *Nat. Electron.* **3**, 5–6 (2020). URL <https://doi.org/10.1038/s41928-019-0363-6>.
- [3] Hara, M. et al. "Super-high-frequency band filters configured with air-gap-type thin-film bulk acoustic resonators". *JJAP* **49**, 07HD13 (2010). URL <https://iopscience.iop.org/article/10.1143/JJAP.49.07HD13/meta>.
- [4] Tsybal, E. Y. & Žutić, I. "Magnon spintronics: Fundamentals of magnon-based computing". in: *Spintronics Handbook: Spin Transport and Magnetism* 247–302 (2019). URL <https://doi.org/10.1201/9780429441189>.
- [5] Bloch, F. "Zur theorie des ferromagnetismus". *Zeitschrift für Physik* **61**, 206–219 (1930). URL <https://doi.org/10.1007/BF01339661>.
- [6] Gurevich, A. G. & Melkov, G. A. *Magnetization oscillations and waves* (CRC press, 2020). URL <https://doi.org/10.1201/9780138748487>.
- [7] Stancil, D. D. & Prabhakar, A. "Spin waves: Theory and applications" (Springer US, New York, 2009), 1 edn. URL <http://books.google.ch/books?id=ehN6-ubvKwoC>.

- [8] Kruglyak, V. V., Demokritov, S. O. & Grundler, D. "Magnonics". *J. Phys. D: Appl. Phys.* **43**, 264001 (2010). URL <https://iopscience.iop.org/article/10.1088/0022-3727/43/26/260301>.
- [9] Serga, A. A., Chumak, A. V. & Hillebrands, B. "YIG magnonics". *Journal of Physics D: Applied Physics* **43**, 264002 (2010). URL <https://iopscience.iop.org/article/10.1088/0022-3727/43/26/264002>.
- [10] Wang, Q. et al. A magnonic directional coupler for integrated magnonic half-adders. *Nat. Electron.* **3**, 765 (2020). URL <https://doi.org/10.1038/s41928-020-00485-6>.
- [11] Brächer, T. & Pirro, P. "An analog magnon adder for all-magnonic neurons". *J. Appl. Phys.* **124** (2018). URL <http://dx.doi.org/10.1063/1.5042417>.
- [12] Wang, Q. et al. "A nonlinear magnonic nano-ring resonator". *npj Comput. Mater.* **6**, 2057–3960 (2020). URL <https://doi.org/10.1038/s41524-020-00465-6>.
- [13] Papp, A., Porod, W. & Csaba, G. "Nanoscale neural network using non-linear spin-wave interference". *Nature Commun.* **12** (2021). URL <https://doi.org/10.1038/s41467-021-26711-z>.
- [14] Chumak, A. V. et al. "Advances in magnetics roadmap on spin-wave computing". *IEEE Trans. Magn.* **58**, 1–72 (2022). URL <https://doi.org/10.1109/TMAG.2022.3149664>.
- [15] Awschalom, D. D. et al. "Quantum engineering with hybrid magnonic systems and materials (invited paper)". *IEEE trans. quantum eng.* **2**, 1–36 (2021). URL <https://doi.org/10.1109/TQE.2021.3057799>.
- [16] Lachance-Quirion, D., Tabuchi, Y., Glorpe, A., Usami, K. & Nakamura, Y. "Hybrid quantum systems based on magnonics". *Appl. Phys. Express* **12**, 070101 (2019). URL <https://iopscience.iop.org/article/10.7567/1882-0786/ab248d/meta>.
- [17] Kittel, C. "On the theory of ferromagnetic resonance absorption". *Phys. Rev.* **73**, 155–161 (1948). URL <https://doi.org/10.1103/PhysRev.73.155>.
- [18] Gerlach, W. & Stern, O. "Der experimentelle nachweis der richtungsquantelung im magnetfeld". *Zeitschrift für Physik* **9**, 349–352 (1922). URL https://ui.adsabs.harvard.edu/link_gateway/1922ZPhy....9.349G/doi:10.1007/BF01326983.
- [19] Milner, R. G. "Nanoscale neural network using non-linear spin-wave interference". *arXiv* (2013). URL <https://arxiv.org/abs/1311.5016>.
- [20] Dirac, P. A. M. "The quantum gravity of the electron". *Proc. R. Soc. A: Math. Phys. Eng. Sci.* **117** (1928).
- [21] Bloch, F. & Rabi, I. I. "Atoms in variable magnetic fields". *Rev. Mod. Phys.* **17**, 237 (1945). URL <https://doi.org/10.1103/RevModPhys.17.237>.
- [22] Ashcroft, N. & Mermin, N. D. "Solid state" (Physics (New York: Holt, Rinehart and Winston) Appendix C, 1976), 1 edn.
- [23] Landau, L. D. & Lifshitz, E. "On the theory of the dispersion of magnetic permeability in ferromagnetic bodies". *Physikalische Zeitschrift der Sowjetunion* **8**, 135 (1935). URL <https://doi.org/10.1016/B978-0-08-036364-6.50008-9>.
- [24] Gilbert, T. L. "A lagrangian formulation of the gyromagnetic equation of the magnetic field". *Phys. Rev.* **100** (1955).
- [25] Holstein, T. & Primakoff, H. "Field dependence of the intrinsic domain magnetization of a ferromagnet". *Phys. Rev.* **58** (1940). URL <https://doi.org/10.1103/PhysRev.58.1098>.
- [26] Dyson, F. J. "General theory of spin-wave interactions". *Phys. Rev.* **102** (1956). URL <https://doi.org/10.1103/PhysRev.102.1217>.
- [27] Griffiths, J. H. E. Anomalous high-frequency resistance of ferromagnetic metals. *Nature* **158**, 670–671 (1946). URL <http://www.nature.com/nature/journal/v158/n4019/pdf/158670a0.pdf>.
- [28] Fleury, P. A., Porto, S. P. S., Cheesman, L. E. & Guggenheim, H. J. "Light scattering by spin waves in FeF₂". *Phys. Rev. Lett.* **17** (1966). URL <https://doi.org/10.1103/PhysRevLett.17.84>.
- [29] Dyson, F. J. "The ferromagnetic faraday effect at microwave frequencies and its applications: The microwave gyrator". *Phys. Rev.* **102** (1956). URL <https://doi.org/10.1103/PhysRev.102.1217>.
- [30] Bloembergen, N. & Damon, R. "Relaxation effects in ferromagnetic resonance". *Phys. Rev.* **85** (1952). URL <https://doi.org/10.1103/PhysRev.85.699>.
- [31] Bloembergen, N. & Wang, S. "Relaxation effects in para- and ferromagnetic resonance". *Phys. Rev.* **93** (1954). URL <https://doi.org/10.1103/PhysRev.93.72>.
- [32] Suhl, H. "The nonlinear behavior of ferrites at high microwave signal levels". *Proc. IRE* **44** (1956). URL <https://doi.org/10.1109/JRPROC.1956.274950>.
- [33] Suhl, H. "The theory of ferromagnetic resonance at high signal powers". *J. Phys. Chem. Solids* **1** (1957). URL [https://doi.org/10.1016/0022-3697\(57\)90010-0](https://doi.org/10.1016/0022-3697(57)90010-0).
- [34] Zavislyak, I. V. & Popov, M. A. "Microwave properties and applications of yttrium iron garnet (YIG) films: Current state of the art and perspectives. In Volkerts, B. D. (ed.) *Yttrium compounds, production and applications* (Nova Science Publishers, Inc, New York, 2011), 1 edn.
- [35] Harris, V. "Modern microwave ferrites". *IEEE Trans. Mag.* **48** (2012). URL <https://doi.org/10.1109/TMAG.2011.2180732>.
- [36] Uebele, G. S. "Characteristics of ferrite microwave limiters". *IRE Trans. Microw. Theory Techniq.* **7** (1959). URL <https://doi.org/10.1109/TMTT.1959.1124618>.
- [37] Eshbachand, J. R. & Damon, R. W. "Surface magnetostatic modes and surface spin waves". *Phys. Rev.* **118** (1960). URL <https://doi.org/10.1103/PhysRev.118.1208>.
- [38] Owens, J. M., Collin, J. H. & Carter, R. L. "System applications of magnetostatic wave devices". *Circuits, Syst. Signal Process* **4** (1985). URL <https://doi.org/10.1007/BF01600088>.
- [39] Stitzer, S. N. & Goldie, H. "System applications of magnetostatic wave devices". *IEEE MTT-S Int. Microw. Symp. Dig.* **326** (1983). URL <https://doi.org/10.1109/MWSYM.1983.1130900>.
- [40] Adam, J. D. "Analog signal processing with microwave magnetics". *Proc. IEEE* **76** (1988). URL <https://doi.org/10.1109/5.4392>.
- [41] Glass, H. L. "Ferrite films for microwave and millimeter-wave devices". *Proc. IEEE* **76** (1988). URL <https://doi.org/10.1109/5.4391>.
- [42] Ishak, W. S. "Magnetostatic wave technology: a review". *Proc. IEEE* **76** (1988). URL <https://doi.org/10.1109/5.4393>.
- [43] Rodrigue, G. P. "A generation of microwave ferrite devices". *Proc. IEEE* **76** (1988). URL <https://doi.org/10.1109/5.4389>.
- [44] Schloemann, E. F. "Circulators for microwave and millimeter-wave integrated circuits". *Proc. IEEE* **76**, 188–200 (1988). URL <https://doi.org/10.1109/5.4394>.
- [45] Bobkov, V. B., Zavislyak, I. V., Zagorodny, V. V. & Romanjuk, V. F. "Microwave filters and multichannel divider based on surface magnetostatic waves". In *12th IEEE Int. Conf. Microw. Telecom. Technol.*, 401–402 (IEEE, 2002). URL <https://doi.org/10.1109/CRMICO.2002.1137289>.
- [46] Hertel, R., Wulfhekel, W. & Kirschner, J. "Domain-wall induced phase shifts in spin waves". *Phys. Rev. Lett.* **93** (2004). URL <https://doi.org/10.1103/PhysRevLett.93.257202>.
- [47] Mahmoud, A. et al. "Introduction to spin wave computing". *J. Appl. Phys.* **128** (2020). URL <https://doi.org/10.1063/5.0019328>.
- [48] Kostylev, M. P., Serga, A. A., Schneider, T., Leven, B. & Hillebrands, B. "Spin-wave logical gates". *Appl. Phys. Lett.* **87** (2005). URL <https://doi.org/10.1063/1.2089147>.
- [49] Schneider, T. et al. "Realization of spin-wave logic gates". *Appl. Phys. Lett.* **92**, 022505 (2008). URL <https://doi.org/10.1063/1.2834714>.
- [50] Lee, K. S. & Kim, S. K. "Conceptual design of spin wave logic gates based on a mach-zehnder-type spin wave interferometer for universal logic functions". *J. Appl. Phys.* **104**, 053909 (2008). URL <https://doi.org/10.1063/1.2975235>.
- [51] Khitun, A., Bao, M. & Wang, K. L. "Magnonic logic circuits". *J. Phys. D: Appl. Phys.* **43**, 264005 (2010). URL <https://iopscience.iop.org/article/10.1088/0022-3727/43/26/264005/meta>.
- [52] Khitun, A. "Multi-frequency magnonic logic circuits for parallel data processing". *J. Appl. Phys.* **111** (2012). URL <https://doi.org/10.1063/1.3689011>.
- [53] Fischer, T. et al. "Experimental prototype of a spin-wave majority gate". *Appl. Phys. Lett.* **110**, 152401 (2017). URL <https://aip.scitation.org/doi/pdf/10.1063/1.4979840>.
- [54] Talmelli, G. et al. "Reconfigurable submicrometer spin-wave majority gate with electrical transducers". *Sci. Adv.* **6**, eabb4042 (2020). URL <https://doi.org/10.1126/sciadv.abb4042>.
- [55] Chumak, A. V., Serga, A. A. & Hillebrands, B. "Magnon transistor for all-magnon data processing". *Nat. Commun.* **5**, 4700 (2014). URL <https://doi.org/10.1038/ncomms5700>.
- [56] Krawczyk, M. & Grundler, D. "Review and prospects of magnonic crystals and devices with reprogrammable band structure". *J. Condens. Matter Phys.* **26**, 123202 (2014). URL <https://iopscience.iop.org/article/10.1088/0953-8984/26/12/123202/meta>.
- [57] Chumak, A. V., Serga, A. A. & Hillebrands, B. "Magnonic crystals for data processing". *J. Phys. D: Appl. Phys.* **50**, 244001 (2017). URL <https://iopscience.iop.org/article/10.1088/1361-6463/aa6a65/meta>.
- [58] Merbouche, H. et al. "Frequency filtering with a magnonic crystal based on nanometer-thick yttrium iron garnet films". *ACS Appl. Nano Mater.* **4**, 121–128 (2021). URL <https://doi.org/10.1021/acsnm.0c02382>.

- [59] Inoue, M. et al. "Investigating the use of magnonic crystals as extremely sensitive magnetic field sensors at room temperature". *Appl. Phys. Lett.* **98** (2011). URL <https://doi.org/10.1063/1.3567940>.
- [60] Metaxas, P. J. et al. "Sensing magnetic nanoparticles using nano-confined ferromagnetic resonances in a magnonic crystal". *Appl. Phys. Lett.* **106** (2015). URL <https://doi.org/10.1063/1.4922392>.
- [61] Nikitin, A. A. et al. "A spin-wave logic gate based on a width-modulated dynamic magnonic crystal". *Appl. Phys. Lett.* **106** (2015). URL <https://doi.org/10.1063/1.4914506>.
- [62] Reed, K., Owens, J. & Carter, R. "Current status of magnetostatic reflective array filters". *Circ. Syst. Signal Pr.* **4**, 157–180 (1985). URL <https://doi.org/10.1007/BF01600078>.
- [63] Demidov, V. E., Demokritov, S. O., Rott, K., Krzysteczko, P. & Reiss, G. "Linear and nonlinear spin-wave dynamics in macro- and microscopic magnetic confined structures". *J. Phys. D: Appl. Phys.* **41**, 164012 (2008). URL <https://iopscience.iop.org/article/10.1088/0022-3727/41/16/164012/meta>.
- [64] Vlaminck, V. & Bailleul, M. "Current-induced spin-wave doppler shift". *Science* **322**, 410–413 (2008). URL <https://doi.org/10.1126/science.1162843>.
- [65] Chumak, A. V. et al. "Spin-wave propagation in a microstructured magnonic crystal". *Appl. Phys. Lett.* **95** (2009). URL <https://doi.org/10.1063/1.3279138>.
- [66] Vlaminck, V. & Bailleul, M. Spin-wave transduction at the submicrometer scale: Experiment and modeling. *Physical Review B—Condensed Matter and Materials Physics* **81**, 014425 (2010).
- [67] Pirro, P. et al. "Spin-wave excitation and propagation in microstructured waveguides of yttrium iron garnet/Pt bilayers". *Appl. Phys. Lett.* **104**, 1–5 (2014). URL <https://doi.org/10.1063/1.4861343>.
- [68] Chumak, A. V., Serga, A. A. & Hillebrands, B. Magnon transistor for all-magnon data processing. *Nature communications* **5**, 4700 (2014).
- [69] Sebastian, T., Schultheiss, K., Obry, B., Hillebrands, B. & Schultheiss, H. Micro-focused brillouin light scattering: imaging spin waves at the nanoscale. *Frontiers in Physics* **3**, 35 (2015).
- [70] Hahn, C. et al. Comparative measurements of inverse spin hall effects and magnetoresistance in yig/pt and yig/ta. *Physical Review B—Condensed Matter and Materials Physics* **87**, 174417 (2013).
- [71] Althammer, M. et al. Quantitative study of the spin hall magnetoresistance in ferromagnetic insulator/normal metal hybrids. *Physical Review B—Condensed Matter and Materials Physics* **87**, 224401 (2013).
- [72] Carsten, D. et al. "Sub-micrometer yttrium iron garnet lpe films with low ferromagnetic resonance losses". *J. Phys. D: Appl. Phys.* **50**, 204005 (2017). URL <https://iopscience.iop.org/article/10.1088/1361-6463/aa6b1c/meta>.
- [73] Dubs, C. et al. "Low damping and microstructural perfection of sub-40nm-thin yttrium iron garnet films grown by liquid phase epitaxy". *Phys. Rev. Materials* **4**, 024416 (2020). URL <https://doi.org/10.1103/PhysRevMaterials.4.024416>.
- [74] Sun, Y. et al. "Growth and ferromagnetic resonance properties of nanometer-thick yttrium iron garnet films". *Appl. Phys. Lett.* **101** (2012). URL <https://doi.org/10.1063/1.4759039>.
- [75] d'Allivy Kelly, O. et al. Inverse spin hall effect in nanometer-thick yttrium iron garnet/pt system. *Applied Physics Letters* **103** (2013).
- [76] Yu, H. et al. "Magnetic thin-film insulator with ultra-low spin wave damping for coherent nanomagnonics". *Sci. Rep.* **4**, 6848 (2014). URL <https://doi.org/10.1038/srep06848>.
- [77] Onbasli, M. C. et al. "Pulsed laser deposition of epitaxial yttrium iron garnet films with low gilbert damping and bulk-like magnetization". *APL Mater.* **2**, 106102 (2014). URL <https://doi.org/10.1063/1.4896936>.
- [78] Schmidt, G., Hauser, C., Trempler, P., Paleschke, M. & Papaioannou, E. T. Ultra thin films of yttrium iron garnet with very low damping: A review. *physica status solidi (b)* **257**, 1900644 (2020).
- [79] Liu, T. et al. "Ferromagnetic resonance of sputtered yttrium iron garnet nanometer films". *J. Appl. Phys.* **115** (2014). URL <https://doi.org/10.1063/1.4852135>.
- [80] Wang, Q. et al. "Spin pinning and spin-wave dispersion in nanoscopic ferromagnetic waveguides". *Phys. Rev. Lett.* **122**, 247202 (2019). URL <https://doi.org/10.1103/PhysRevLett.122.247202>.
- [81] Heinz, B. et al. "Propagation of spin-wave packets in individual nanosized yttrium iron garnet magnonic conduits". *Nano Letters* **20**, 4220–4227 (2020). URL <https://doi.org/10.1021/acs.nanolett.0c00657>.
- [82] Bailleul, M., Olligs, D. & Fermon, C. "Propagating spin wave spectroscopy in a permalloy film: A quantitative analysis". *Appl. Phys. Lett.* **83**, 972–974 (2003). URL <https://doi.org/10.1063/1.1597745>.
- [83] Vanderveken, F. et al. "Lumped circuit model for inductive antenna spin-wave transducers. *Sci. Rep.* **12**, 3796 (2022). URL <https://doi.org/10.1038/s41598-022-07625-2>.
- [84] Connelly, D. A. et al. "Efficient electromagnetic transducers for spin-wave devices". *Sci. Rep.* **11**, 18378 (2021). URL <https://doi.org/10.1038/s41598-021-97627-3>.
- [85] Mahmoud, A. et al. "Fan-out enabled spin wave majority gate". *Aip Advances* **10** (2020). URL <https://doi.org/10.1063/1.5134690>.
- [86] Hirohata, A. et al. "Review on spintronics: Principles and device applications". *J. Magn. Magn. Mater.* **509**, 166711 (2020). URL <https://doi.org/10.1016/j.jmmm.2020.166711>.
- [87] Talmelli, G. et al. "Spin-wave emission by spin-orbit-torque antennas". *Phys. Rev. Appl.* **10**, 044060 (2018). URL <https://doi.org/10.1103/PhysRevApplied.10.044060>.
- [88] Dai, S., Bhawe, S. A. & Wang, R. "Octave-tunable magnetostatic wave YIG resonators on a chip. *IEEE Trans. Ultrason. Ferroelectr. Freq. Control* **67**, 2454–2460 (2020). URL <https://doi.org/10.1109/TUFFC.2020.3000055>.
- [89] Feng, Y., Tiwari, S., Bhawe, S. A. & Wang, R. "Micromachined tunable magnetostatic forward volume wave bandstop filter". *IEEE MWTL* **33**, 807–810 (2023). URL <https://doi.org/10.1109/LMWT.2023.3267449>.
- [90] Lachance-Quirion, D. et al. Entanglement-based single-shot detection of a single magnon with a superconducting qubit. *Science* **367**, 425–428 (2020).
- [91] Karenowska, A. D., Patterson, A. D., Peterer, M. J., Magnússon, E. B. & Leek, P. J. Excitation and detection of propagating spin waves at the single magnon level. *arXiv preprint arXiv:1502.06263* (2015).
- [92] Knauer, S. et al. "Propagating spin-wave spectroscopy in a liquid-phase epitaxial nanometer-thick YIG film at millikelvin temperatures". *J. Appl. Phys.* **133**, 143905 (2023). URL <https://doi.org/10.1063/5.0137437>.
- [93] Li, Y. et al. Hybrid magnonics: Physics, circuits, and applications for coherent information processing. *Journal of Applied Physics* **128** (2020).
- [94] Lachance-Quirion, D., Tabuchi, Y., Gloppe, A., Usami, K. & Nakamura, Y. Hybrid quantum systems based on magnonics. *Applied Physics Express* **12**, 070101 (2019).
- [95] Xu, D. et al. Quantum control of a single magnon in a macroscopic spin system. *Physical Review Letters* **130**, 193603 (2023).
- [96] Yuan, H., Cao, Y., Kamra, A., Duine, R. A. & Yan, P. Quantum magnonics: When magnon spintronics meets quantum information science. *Physics Reports* **965**, 1–74 (2022).
- [97] Li, Y. et al. Hybrid-magnon quantum devices: Strategies and approaches. In *2022 International Electron Devices Meeting (IEDM)*, 14–6 (IEEE, 2022).
- [98] Wang, Q., Chumak, A. V. & Pirro, P. "Inverse-design magnonic devices". *Nat. Commun* **12**, 2636 (2021). URL <https://doi.org/10.1038/s41467-021-22897-4>.
- [99] Chumak, A. et al. Experimental realisation of a universal inverse-design magnonic device. *arXiv preprint arXiv:2403.17724* (2024).
- [100] Geller, S. & Gilleo, M. "Structure and ferrimagnetism of yttrium and rare-earth-iron garnets". *Acta Crystallogr.* **10**, 239–239 (1957). URL <https://doi.org/10.1107/S0365110X57000729>.
- [101] Glass, H. & Elliot, M. "Attainment of the intrinsic FMR linewidth in yttrium iron garnet films grown by liquid phase epitaxy". *J. Cryst. Growth* **34**, 285–288 (1976). URL [https://doi.org/10.1016/0022-0248\(76\)90141-X](https://doi.org/10.1016/0022-0248(76)90141-X).
- [102] Cherepanov, V., Kolokolov, I. & L'vov, V. "The saga of yig: Spectra, thermodynamics, interaction and relaxation of magnons in a complex magnet". *Phys. Rep.* **229**, 81–144 (1993). URL [https://doi.org/10.1016/0370-1573\(93\)90107-O](https://doi.org/10.1016/0370-1573(93)90107-O).
- [103] Serga, A. A., Chumak, A. V. & Hillebrands, B. "YIG magnonics". *J. Phys. D: Appl. Phys.* **43**, 264002 (2010). URL <https://iopscience.iop.org/article/10.1088/0022-3727/43/26/264002>.
- [104] Chumak, A. V., Vasyuchka, V. I., Serga, A. A. & Hillebrands, B. "Magnon spintronics. *Nature Physics* **11**, 1505–1549 (2015). URL <https://doi.org/10.1038/nphys3347>.
- [105] Barman, A. et al. "The 2021 magnonics roadmap". *J. Condens. Matter Phys.* **33**, 413001 (2021). URL <https://iopscience.iop.org/article/10.1088/1361-648X/abec1a/meta>.
- [106] Dutta, S. et al. "Non-volatile clocked spin wave interconnect for beyond-cmos nanomagnet pipelines". *Scientific reports* **5**, 9861 (2015). URL <https://doi.org/10.1038/srep09861>.

- [107] Khitun, A. "Magnonic holographic devices for special type data processing". *J. Appl. Phys.* **113** (2013). URL <https://doi.org/10.1063/1.4802656>.
- [108] Gertz, F., Kozhevnikov, A. V., Filimonov, Y. A., Nikonov, D. E. & Khitun, A. "Magnonic holographic memory: From proposal to device". *IEEE JXDC* **1**, 67–75 (2015). URL <https://ieeexplore.ieee.org/abstract/document/7174516>.
- [109] Dieny, B. et al. "Opportunities and challenges for spintronics in the microelectronics industry". *Nat. Electron.* **3**, 446 (2020). URL <https://doi.org/10.1038/s41928-020-0461-5>.
- [110] Serga, A. A., Demokritov, S. O., Hillebrands, B. & Slavin, A. N. "Self-generation of two-dimensional spin-wave bullets". *Phys. Rev. Lett.* **92**, 117203 (2004). URL <https://doi.org/10.1103/PhysRevLett.92.117203>.
- [111] Schneider, A. A., T and Serga et al. "Nondiffractive subwavelength wave beams in a medium with externally controlled anisotropy". *Phys. Rev. Lett.* **104**, 197203 (2010). URL <https://doi.org/10.1103/PhysRevLett.104.197203>.
- [112] Serga, A. A. et al. "Parametric generation of forward and phase-conjugated spin-wave bullets in magnetic films". *Phys. Rev. Lett.* **94**, 167202 (2005). URL <https://doi.org/10.1103/PhysRevLett.94.167202>.
- [113] Schneider, M. et al. "Control of the Bose-Einstein condensation of magnons by the spin Hall effect". *Phys. Rev. Lett.* **127**, 237203 (2021). URL <https://doi.org/10.1103/PhysRevLett.127.237203>.
- [114] Schneider, M. et al. "Stabilization of a nonlinear magnonic bullet co-existing with a Bose-Einstein condensate in a rapidly cooled magnonic system driven by spin-orbit torque". *Phys. Rev. B* **104**, L140405 (2021). URL <https://doi.org/10.1103/PhysRevB.104.L140405>.
- [115] Schneider, M. et al. "Bose-Einstein condensation of quasiparticles by rapid cooling". *Nat. Nanotechnol.* **15**, 457 (2020). URL <https://doi.org/10.1038/s41565-020-0671-z>.
- [116] Heinz, B. et al. "Parametric generation of spin waves in nanoscaled magnonic conduits". *Phys. Rev. B* **105** (2022). URL <https://doi.org/10.1103/PhysRevB.105.144424>.
- [117] Rezende, S. M. *Fundamentals of Magnonics*, vol. 969 (Springer International Publishing, 2020).
- [118] Ganguly, A. K. & Webb, D. C. "Radiation resistance of microstrip excited magnetostatic surface waves". In *1975 IEEE-MTT-S IMS*, 368–370 (IEEE, 1975). URL <https://doi.org/10.1109/MWSYM.1975.1123398>.
- [119] Vaňatka, M. et al. Spin-wave dispersion measurement by variable-gap propagating spin-wave spectroscopy. *Physical Review Applied* **16**, 054033 (2021).
- [120] Zhang, Y. et al. "Antenna design for propagating spin wave spectroscopy in ferromagnetic thin films". *J. Magn. Magn. Mater.* **450**, 24–28 (2018). URL <https://doi.org/10.1016/j.jmmm.2017.04.048>.
- [121] Demidov, V. E., Urazhdin, S. & Demokritov, S. O. Direct observation and mapping of spin waves emitted by spin-torque nano-oscillators. *Nature materials* **9**, 984–988 (2010).
- [122] Madami, M. et al. Direct observation of a propagating spin wave induced by spin-transfer torque. *Nature nanotechnology* **6**, 635–638 (2011).
- [123] Chen, T. et al. Spin-torque and spin-hall nano-oscillators. *Proceedings of the IEEE* **104**, 1919–1945 (2016).
- [124] Wu, M., Kalinikos, B. A., Krivosik, P. & Patton, C. E. Fast pulse-excited spin waves in yttrium iron garnet thin films. *Journal of applied physics* **99** (2006).
- [125] Chen, C., Barra, A., Mal, A., Carman, G. & Sepulveda, A. Voltage induced mechanical/spin wave propagation over long distances. *Applied Physics Letters* **110** (2017).
- [126] Tserkovnyak, Y., Brataas, A. & Bauer, G. E. Spin pumping and magnetization dynamics in metallic multilayers. *Physical Review B* **66**, 224403 (2002).
- [127] Serha, R. O. et al. Low-damping spin-wave transmission in yig/pt-interfaced structures. *Advanced Materials Interfaces* **9**, 2201323 (2022).
- [128] Bunyaev, S. A. et al. Spin-wave relaxation by eddy currents in y3fe5o12/pt bilayers and a way to suppress it. *Physical Review Applied* **14**, 024094 (2020).
- [129] Yao, Z., Wang, Y. E., Keller, S. & Carman, G. P. "Bulk acoustic wave-mediated multiferroic antennas: Architecture and performance bound". *IEEE Trans. Antennas Propag.* **63**, 3335–3344 (2015). URL <https://doi.org/10.1109/TAP.2015.2431723>.
- [130] Domann, J. P. & Carman, G. P. "Strain powered antennas". *J. Appl. Phys.* **121** (2017). URL <https://doi.org/10.1063/1.4975030>.
- [131] Erdélyi, R. et al. Design rules for low-insertion-loss magnonic transducers. *arXiv preprint arXiv:2410.14370* (2024).
- [132] Jungfleisch, M. B. et al. "thickness and power dependence of the spin-pumping effect in Y3Fe5O12/Pt heterostructures measured by the inverse spin Hall effect". *Phys. Rev. B* **91**, 134407 (2015). URL <https://doi.org/10.1103/PhysRevB.91.134407>.
- [133] Breitbach, D. et al. Nonlinear erasing of propagating spin-wave pulses in thin-film ga: Yig. *Applied Physics Letters* **124** (2024).
- [134] Serga, A. et al. Parametrically stimulated recovery of a microwave signal stored in standing spin-wave modes of a magnetic film. *Physical review letters* **99**, 227202 (2007).
- [135] Wang, Q., Csaba, G., Verba, R., Chumak, A. V. & Pirro, P. Nanoscale magnonic networks. *Physical Review Applied* **21**, 040503 (2024).
- [136] Suess, D. et al. Time resolved micromagnetics using a preconditioned time integration method. *Journal of Magnetism and Magnetic Materials* **248**, 298–311 (2002).
- [137] Abert, C. Micromagnetics and spintronics: models and numerical methods. *The European Physical Journal B* **92**, 1–45 (2019).
- [138] Bruckner, F., Koraltan, S., Abert, C. & Suess, D. magnum. np: a pytorch based gpu enhanced finite difference micromagnetic simulation framework for high level development and inverse design. *Scientific Reports* **13**, 12054 (2023).
- [139] Kakay, A., Westphal, E. & Hertel, R. Speedup of fem micromagnetic simulations with graphical processing units. *IEEE transactions on magnetics* **46**, 2303–2306 (2010).
- [140] Chang, R., Li, S., Lubarda, M., Livshitz, B. & Lomakin, V. Fastmag: Fast micromagnetic simulator for complex magnetic structures. *Journal of Applied Physics* **109** (2011).
- [141] Dvornik, M., Vansteenkiste, A. & Van Waeyenberge, B. Thermodynamically self-consistent non-stochastic micromagnetic model for the ferromagnetic state. *Applied Physics Letters* **105** (2014).
- [142] D'Aquino, M. & et al. A novel formulation for the numerical computation of magnetization modes in complex micromagnetic systems. *J. Comput. Phys.* **228**, 6130 (2009).
- [143] Bruckner, F. & et al. Large scale finite-element simulation of micromagnetic thermal noise. *J. Magn. Magn. Mater.* **475**, 408 (2019).
- [144] Perna, S. & et al. Computational micromagnetics based on normal modes: Bridging the gap between macrospin and full spatial discretization. *J. Magn. Magn. Mater.* **546**, 168683 (2022).
- [145] FD, M. Magnum fd - micromagnetic simulation software. <http://micromagnetics.org/magnum/fd/> (2024). Accessed: 2024-11-20.
- [146] MuMax. Mumax - micromagnetic simulation software. <https://mumax.github.io/> (2024). Accessed: 2024-11-20.
- [147] Software, T. Tetrax - micromagnetic simulation software. <https://www.tetrax.software/> (2024). Accessed: 2024-11-20.
- [148] Spintronics, B. Boris spintronics - research on spintronics and related technologies. <https://www.boris-spintronics.uk/> (2024). Accessed: 2024-11-20.
- [149] Abert, C. et al. Neuralmag: an open-source nodal finite-difference code for inverse micromagnetics. *arXiv* (2024). URL <https://arxiv.org/abs/2411.11725>.
- [150] NIST. Oommf - object oriented micromagnetic framework. <https://math.nist.gov/oommf/> (2024). Accessed: 2024-11-20.
- [151] Kiechle, M. et al. Experimental demonstration of a spin-wave lens designed with machine learning. *IEEE Magnetics Letters* **13**, 1–5 (2022).
- [152] Voronov, A. et al. Inverse-design topology optimisation of magnonic devices using level-set and adjoint-state methods. *Submitted* (2024). Submitted for publication.
- [153] Palmer, W. et al. A bright future for integrated magnetics: Magnetic components used in microwave and mm-wave systems, useful materials, and unique functionalities. *IEEE Microwave Magazine* **20**, 36–50 (2019).
- [154] Gladii, O., Haidar, M., Henry, Y., Kostylev, M. & Bailleul, M. Frequency nonreciprocity of surface spin wave in permalloy thin films. *Physical Review B* **93**, 054430 (2016).
- [155] Brächer, T., Boulle, O., Gaudin, G. & Pirro, P. Creation of unidirectional spin-wave emitters by utilizing interfacial dzyaloshinskii-moriya interaction. *Physical Review B* **95**, 064429 (2017).
- [156] Chen, J. et al. Excitation of unidirectional exchange spin waves by a nanoscale magnetic grating. *Physical Review B* **100**, 104427 (2019).
- [157] Grassi, M. et al. Slow-wave-based nanomagnonic diode. *Physical Review Applied* **14**, 024047 (2020).
- [158] Gallardo, R. et al. Reconfigurable spin-wave nonreciprocity induced by dipolar interaction in a coupled ferromagnetic bilayer. *Physical Review Applied* **12**, 034012 (2019).
- [159] Wojewoda, O. et al. Unidirectional propagation of zero-momentum magnons. *Applied Physics Letters* **125** (2024).

- [160] Serha, R. O. et al. Magnetic anisotropy and ggg substrate stray field in yig films down to millikelvin temperatures. *npj Spintronics* **2**, 29 (2024).
- [161] Schmoll, D. et al. Wavenumber-dependent magnetic losses in yig-ggg heterostructures at millikelvin temperatures. *arXiv preprint arXiv:2411.13414* (2024). URL <https://arxiv.org/abs/2411.13414>.
- [162] Böttcher, T. et al. "Fast long-wavelength exchange spin waves in partially compensated Ga:YIG". *Appl. Phys. Lett.* **120**, 102401 (2022). URL <https://doi.org/10.1063/5.0082724>.
- [163] Carmiggelt, J. J., Dreijer, O. C., Dubs, C., Surzhenko, O. & Van Der Sar, T. "Electrical spectroscopy of the spin-wave dispersion and bistability in gallium-doped yttrium iron garnet". *Appl. Phys. Lett.* **119** (2021). URL <https://doi.org/10.1063/5.0070796>.
- [164] Zhang, G. & Jiang, Y. "A novel CMOS hexaferrite circulator with 25 ghz operating frequency". *AIP Advances* **11** (2021). URL <https://doi.org/10.1063/5.0028225>.
- [165] Zuo, X., How, H., Somu, S. & Vittoria, C. "Self-biased circulator/isolator at millimeter wavelengths using magnetically oriented polycrystalline strontium M-type hexaferrite". *IEEE Trans. Magn.* **39**, 3160–3162 (2003). URL <https://doi.org/10.1109/TMAG.2003.816043>.
- [166] Song, Y.-Y., Sun, Y., Lu, L., Bevivino, J. & Wu, M. "Self-biased planar millimeter wave notch filters based on magnetostatic wave excitation in barium hexagonal ferrite thin films". *Appl. Phys. Lett.* **97** (2010). URL <https://doi.org/10.1063/1.3504256>.
- [167] Popov, M. et al. "Nonlinear magnetolectric effects in Y-type hexaferrite microwave resonators". *J. Appl. Phys.* **128** (2020). URL <https://doi.org/10.1063/5.0021593>.
- [168] Wang, S. G., Yoon, S. D. & Vittoria, C. "Microwave and magnetic properties of double-sided hexaferrite films on (111) magnesium oxide substrates". *J. Appl. Phys.* **92**, 6728–6732 (2002). URL <https://doi.org/10.1063/1.1517749>.
- [169] Malkinski, L. "Advanced magnetic materials" (BoD–Books on Demand, 2012), 1 edn.
- [170] Gillette, S. M. et al. "Active tuning of a microstrip hairpin-line microwave bandpass filter on a polycrystalline yttrium iron garnet substrate using small magnetic fields". *J. Appl. Phys.* **109** (2011). URL <https://doi.org/10.1063/1.3556696>.
- [171] Elliott, S. S., Nieh, S. T. K. & Craig, R. A. "Broadband, frequency selective limiters in the 4-16 GHz range". In *1974 4th European Microwave Conference*, 521–525 (IEEE, 1974). URL <https://doi.org/10.1109/EUMA.1974.332104>.
- [172] Yang, M. et al. "X-band ferrite microstrip limiter based on improved nonlinear loss model for high-power microwave application". *IEEE MWTL* **32**, 1015–1018 (2022). URL <https://doi.org/10.1109/LMWC.2022.3165555>.
- [173] Adam, J. D. & Stitzer, S. N. "MSW frequency selective limiters at UHF". *IEEE Trans. Magn.* **40**, 2844–2846 (2004). URL <https://doi.org/10.1109/TMAG.2004.832117>.
- [174] Yamanouchi, K., Qureshi, J. A. & Odagawa, H. "5-15 GHz range surface acoustic wave filters using electrode thickness difference type and new reflector bank type of unidirectional interdigital transducers". In *1997 IEEE Ultrason. Symp. Proceed.: Intern. Sympos.*, vol. 1, 61–64 (IEEE, 1997). URL <https://doi.org/10.1109/ULTSYM.1997.662980>.
- [175] Kapilevich, B. Y. & Safonov, S. Y. "Tunable microwave ferrite filter for receiving-transmitting mobile communications systems". In *IEEE Int. Symp. Electromagn. Compat.*, 537–541 (IEEE, 1990). URL <https://doi.org/10.1109/ISEMC.1990.252826>.
- [176] Ishak, W. S. & Chang, K.-W. "Tunable microwave resonators using magnetostatic wave in yig films". *IEEE Trans. Microw. Theory Techn.* **34**, 1383–1393 (1986). URL <https://doi.org/10.1109/TMTT.1986.1133553>.
- [177] Ishak, W. S. "Microwave signal processing using magnetostatic wave devices". In *IEEE Int. Ultrason. Symp.*, 152–163 (IEEE, 1984). URL <https://doi.org/10.1109/ULTSYM.1984.198281>.
- [178] Wu, J., Yang, X., Beguhn, S., Lou, J. & Sun, N. X. "Nonreciprocal tunable low-loss bandpass filters with ultra-wideband isolation based on magnetostatic surface wave". *IEEE Trans. Microw. Theory Techn.* **60**, 3959–3968 (2012). URL <https://doi.org/10.1109/TMTT.2012.2222661>.
- [179] Hartemann, P. Magnetostatic wave planar yig devices. *IEEE Transactions on Magnetics* **20**, 1272–1277 (1984).
- [180] Djafari-Rouhani, B., Al-Wahsh, H., Akjouj, A. & Dobrzynski, L. One-dimensional magnonic circuits with size-tunable band gaps and selective transmission. In *Journal of Physics: Conference Series*, vol. 303, 012017 (IOP Publishing, 2011).
- [181] Zhu, Y., Chi, K. & Tsai, C. Magnonic crystals-based tunable microwave phase shifters. *Applied Physics Letters* **105** (2014).
- [182] Bankowski, E. et al. Magnonic crystal as a delay line for low-noise auto-oscillators. *Applied Physics Letters* **107** (2015).
- [183] Frey, P. et al. Reflection-less width-modulated magnonic crystal. *Communications Physics* **3**, 17 (2020).
- [184] Kalinikos, B. A. & Ustinov, A. B. "Nonlinear spin waves in magnetic films and structures: physics and devices". In *Solid State Phys.*, vol. 64, 193–235 (Elsevier, 2013). URL <https://doi.org/10.1016/B978-0-12-408130-7.00007-1>.
- [185] Krug, J. Microwave tapped delay line with amplitude weighting and electronic phase tuning. *IEEE Transactions on Magnetics* **20**, 1244–1245 (1984).
- [186] Hansen, U.-H., Demidov, V. E. & Demokritov, S. O. Dual-function phase shifter for spin-wave logic applications. *Applied Physics Letters* **94** (2009).
- [187] Au, Y., Dvornik, M., Dmytriiev, O. & Kruglyak, V. Nanoscale spin wave valve and phase shifter. *Applied Physics Letters* **100** (2012).
- [188] Adkins, L. et al. Electronically variable time delays using cascaded magnetostatic delay lines. *Journal of Applied Physics* **55**, 2518–2520 (1984).
- [189] Bajpai, S. N., Weinert, R. W. & Adam, J. D. "Variable magnetostatic wave delay lines". *J. Appl. Phys.* **58**, 990–996 (1985). URL <https://doi.org/10.1063/1.336147>.
- [190] Adam, J. D. Mitigate the interference: Nonlinear frequency selective ferrite devices. *IEEE Microwave Magazine* **15**, 45–56 (2014).
- [191] Shukla, M. et al. Adaptive interference mitigation using frequency-selective limiters over gps band for automotive applications. In *2020 IEEE Intern. Symp. EM Compat. Signal/Power Integr. (EMCSI)*, 614–618 (IEEE, 2020).
- [192] Elliott, S. S. "A broadband ferrite limiter". In *AIP Conference Proceedings*, vol. 18, 1273–1277 (American Institute of Physics, 1974). URL <https://doi.org/10.1063/1.2947257>.
- [193] Adam, J. D. & Stitzer, S. N. "A magnetostatic wave signal-to-noise enhancer". *Appl. Phys. Lett.* **36**, 485–487 (1980). URL <https://doi.org/10.1063/1.91516>.
- [194] Kuki, T. & Nomoto, T. "(MSSW/BVW) hybrid modes for a signal-to-noise enhancer". *Electron. Comm. Jpn. (Part II: Electron.)* **81**, 30–37 (1998). URL [https://doi.org/10.1002/\(SICI\)1520-6432\(199809\)81:9%3C30::AID-ECJB4%3E3.0.CO;2-4](https://doi.org/10.1002/(SICI)1520-6432(199809)81:9%3C30::AID-ECJB4%3E3.0.CO;2-4).
- [195] Davidková, K. et al. Nanoscaled spin-wave frequency selective limiter (fsl) for 5g. Submitted (2024). Submitted for publication.
- [196] Wang, Q. et al. "Deeply nonlinear excitation of self-normalized short spin waves". *Sci. Adv.* **9**, eadg4609 (2023). URL <https://doi.org/10.1126/sciadv.adg4609>.
- [197] Wang, Q. et al. All-magnonic repeater based on bistability. *Nature Communications* **15**, 7577 (2024).
- [198] Wang, Q. et al. Nanoscale spin-wave wake-up receiver. *Applied Physics Letters* **115** (2019).
- [199] Wang, Q. et al. Realization of a nanoscale magnonic directional coupler for all-magnon circuits. *arxiv:1905.12353* (2019).
- [200] Zhu, X. et al. Autonomous micro-magnet based systems for highly efficient magnetic separation. *Applied Physics Letters* **99**, 232504 (2011). URL <https://pubs.aip.org/aip/apl/article-abstract/99/23/232504/282288/Autonomous-micro-magnet-based-systems-for-highly?redirectedFrom=fulltext>.
- [201] Keller, F. O., Haettel, R., Devillers, T. & Dempsey, N. M. Batch fabrication of 50 μm -thick anisotropic nd–fe–b micro-magnets. *IEEE Transactions on Magnetics* **58**, 1–5 (2021).
- [202] Kovacs, A. et al. Physics-informed machine learning combining experiment and simulation for the design of neodymium-iron-boron permanent magnets with reduced critical-elements content. *Frontiers in Materials* **9**, 1094055 (2023).
- [203] Wikipedia contributors. Chiplet (2024). URL <https://en.wikipedia.org/wiki/Chiplet#:~:text=A%20chiplet%20is%20a%20tiny,%22Lego%2Dlike%22%20assembly>.
- [204] Guinness World Records. Highest clock frequency achieved by a silicon processor (2011). URL <https://www.guinnessworldrecords.com/world-records/98281-highest-clock-frequency-achieved-by-a-silicon-processor>.
- [205] Brataas, A., van Wees, B., Klein, O., de Loubens, G. & Viret, M. "Spin insulator". *Phys. Rep.* **885**, 1–27 (2020). URL <https://doi.org/10.1016/j.physrep.2020.08.006>.
- [206] Wigen, P. E. "Nonlinear phenomena and chaos in magnetic materials" (Singapore: World Scientific, 1994).
- [207] Freire, M. J., Marques, R. & Medina, F. "A new method for the computation of the insertion loss of magnetostatic-surface wave transducers". In *2003 33rd European Microwave Conference*, 563–566 (IEEE, 2003). URL <https://doi.org/10.1109/EUMA.2003.341015>.

- [208] Chumak, A. V. et al. "Direct detection of magnon spin transport by the inverse spin Hall effect". *Appl. Phys. Lett.* **100** (2012). URL <https://doi.org/10.1063/1.3689787>.
- [209] Ishak, W. "Magnetostatic surface wave devices for UHF and L band applications". *IEEE Trans. Magn.* **19**, 1880–1882 (1983). URL <https://doi.org/10.1109/TMAG.1983.1062691>.
- [210] Adam, J. D., Daniel, M. R. & Okeeffe, T. W. "Magnetostatic wave devices". *MWJ* **25**, 95–99 (1982). URL <https://ui.adsabs.harvard.edu/abs/1982MiJo...25...95A/abstract>.
- [211] Sethares, J. C., Owens, J. M. & Smith, C. V. "MSW nondispersive, electronically tunable time delay elements". *Electron. Lett.* **16**, 825–826 (1980). URL https://digital-library.theiet.org/content/journals/10.1049/el_19800586.
- [212] Bajpai, S., Weinert, R. & Adam, J. "Delay control via the bias field angle in YIG films". *IEEE Trans. Magn.* **19**, 1877–1879 (1983). URL <https://doi.org/10.1109/TMAG.1983.1062689>.
- [213] Bunyaev, S. A. et al. "Engineered magnetization and exchange stiffness in direct-write Co-Fe nanoelements". *Appl. Phys. Lett.* **118** (2021). URL <https://doi.org/10.1063/5.0036361>.
- [214] Kobljanskyj, Y. V., Melkov, G. A., Pan, V. M., Tiberkevich, V. S. & Slavin, A. N. "Formation and propagation of dipolar spin wave envelope solitons under the influence of parametric pumping". *IEEE Trans. Magn.* **38**, 3099–3101 (2002). URL <https://doi.org/10.1109/TMAG.2002.802479>.
- [215] Fetisov, Y. K., Kabos, P. & Patton, C. E. "Active magnetostatic wave delay line". *IEEE Trans. Magn.* **34**, 259–271 (1998). URL <https://doi.org/10.1109/20.650254>.
- [216] Kalinikos, B. A., Kovshikov, N. G. & Slavin, A. N. "Envelope solitons of highly dispersive and low dispersive spin waves in magnetic films". *J. Appl. Phys.* **69**, 5712–5717 (1991). URL <https://doi.org/10.1063/1.347896>.